

# Convergent origin and accelerated evolution of vesicle-associated RhoGAP proteins in two unrelated parasitoid wasps

Dominique Colinet<sup>\*1</sup>, Fanny Cavigliasso<sup>1</sup>, Matthieu Leobold<sup>2</sup>, Appoline Pichon<sup>3</sup>, Serge Urbach<sup>3</sup>, Dominique Cazes<sup>1</sup>, Marine Pouillet<sup>1</sup>, Maya Belghazi<sup>4</sup>, Anne-Nathalie Volkoff<sup>3</sup>, Jean-Michel Drezen<sup>2</sup>, Jean-Luc Gatti<sup>1</sup>, and Marylène Poirié<sup>1</sup>

<sup>1</sup> Université Côte d'Azur, INRAE, CNRS, ISA, 06903 Sophia Antipolis, France

<sup>2</sup> Institut de Recherche sur la Biologie de l'Insecte (IRBI), UMR 7261, CNRS - Université de Tours, Tours, France

<sup>3</sup> DGIMI, Univ Montpellier, INRAE, 34095 Montpellier, France

<sup>4</sup> Aix Marseille Université, CNRS, Plateforme Protéomique, IMM FR3479, Marseille Protéomique (MaP), 13402 Marseille, France

\*Corresponding author

Correspondence: dominique.colinet@inrae.fr

## ABSTRACT

Animal venoms and other protein-based secretions that perform a variety of functions, from predation to defense, are highly complex cocktails of bioactive compounds. Gene duplication, accompanied by modification of the expression and/or function of one of the duplicates under the action of positive selection, followed by further duplication to produce multigene families of toxins is a well-documented process in venomous animals. This evolutionary model has been less described in parasitoid wasps, which use maternal fluids, including venom, to protect their eggs from encapsulation by the host immune system. Here, we evidence the convergent recruitment and accelerated evolution of two multigene families of RhoGAPs presumably involved in virulence in two unrelated parasitoid wasp species, *Leptopilina bouvardi* (Figitidae) and *Venturia canescens* (Icheumonidae). In both species, these RhoGAPs are associated with vesicles that act as transport systems to deliver virulence factors, but are produced in different tissues: the venom gland in *Leptopilina* sp. and the ovarian calyx in *V. canescens*. We show that the gene encoding the cellular RacGAP1 is at the origin of the virulent RhoGAP families found in *Leptopilina* sp. and *V. canescens*. We also show that both RhoGAP families have undergone evolution under positive selection and that almost all of these RhoGAPs lost their GAP activity and GTPase binding ability due to substitutions in key amino acids. These results suggest an accelerated evolution and functional diversification of these vesicle-associated RhoGAPs in the two phylogenetically distant parasitoid species. The potential new function(s) and the exact mechanism of action of these proteins in host cells remain to be elucidated.

**Keywords:** parasitoids, venom and other secretions, RhoGAP multigene family, evolution, gene duplication, positive selection

45 Gene duplication is recognized as an important evolutionary process because it drives functional  
46 novelty (Chen et al., 2013; Long et al., 2013). The importance of gene duplication for genetic and functional  
47 innovation was popularized by Ohno, who postulated that one of the two duplicate copies could evolve a  
48 new function through mutation, while the other would be responsible for the ancestral function (Ohno  
49 1970). Since then, there have been numerous examples of duplication followed by neofunctionalization of  
50 one of the two paralogs with critical roles in fundamental biological processes (Kaessmann 2010; Magadum  
51 et al. 2013, Copley 2020). In particular, the formation of multigene families by repeated gene duplication  
52 is a widely studied evolutionary process in several groups of venomous animals (Fry et al., 2009; Wong &  
53 Belov 2012; Casewell et al., 2013), but also in some parasites (Akhter et al., 2012; Arisue et al., 2020). Such  
54 repeated duplication events of venomous or virulence protein-coding genes are often accompanied by  
55 significant copy divergence through positive selection, allowing the acquisition of new functions. In this  
56 work, we studied the process of accelerated evolution by duplication and divergence of two multigene  
57 families encoding RhoGAPs presumably involved in virulence in two phylogenetically distant parasitoid  
58 wasp species, *Leptopilina* species of the family Figitidae and *Venturia canescens* of the family  
59 Ichneumonidae.

60 The development of parasitoid wasps occurs at the expense of another arthropod, whose tissues are  
61 consumed by the parasitoid larvae, usually resulting in the host death (Godfray 1994). For endoparasitoids  
62 that lay eggs inside the host body, the host immune defense against parasitoids is usually based on the  
63 formation of a multicellular melanized capsule around the parasitoid egg, resulting in its death (Carton et  
64 al., 2008). To escape encapsulation, parasitoids have evolved several strategies, the main one being the  
65 injection of maternal fluids together with the egg into the host at the time of oviposition (Pennacchio &  
66 Strand 2006; Poirié et al., 2009). These maternal fluids contain (i) proteins synthesized in the venom glands  
67 (Asgari & Rivers 2010; Poirié et al., 2014), some of which, as in *Leptopilina*, can be associated with  
68 extracellular vesicles called venosomes and allow their transport to the targeted immune cells (Gatti et al.,  
69 2012; Wan et al., 2019), (ii) proteins synthesized in the ovarian calyx cells and associated with particles of  
70 viral origin devoid of nucleic acid and named virus-like particles (VLPs) as in *V. canescens* (Reineke et al.,  
71 2006; Gatti et al., 2012; Pichon et al., 2015), and (iii) polydnviruses (PDVs) integrated into the parasitoid  
72 genome and found in some groups of parasitoids belonging to the families Braconidae and Ichneumonidae  
73 (Drezen et al., 2014). Like VLPs, PDVs are synthesized in the ovarian calyx cells and are present in the  
74 ovarian fluid along with the egg. These particles are unique in that they are formed by the integrated viral  
75 machinery, but carry circular double-stranded DNA molecules that contain virulence genes that will be  
76 expressed in the host cells (Drezen et al., 2014). The process of accelerated evolution by duplication and  
77 divergence has been described for some of these virulence genes carried by PDVs, suggesting functional  
78 diversification of the proteins produced (Serbielle et al., 2008; Serbielle et al., 2012; Jancek et al., 2013).

79 *Leptopilina boulardi* is a parasitoid wasp of *Drosophila* for which two lines have been well characterized  
80 (Dubuffet et al., 2009). The ISm line of *L. boulardi* is highly virulent against *Drosophila melanogaster* but is  
81 unable to develop in *Drosophila yakuba* whereas the ISy line can develop in both *Drosophila* species but its  
82 success depends on the resistance/susceptibility of the host (Dubuffet et al., 2009). One of the most  
83 abundant proteins in the venom of the *L. boulardi* ISm line is LbmGAP (previously named LbGAP), which  
84 belongs to the Rho GTPase activating protein (RhoGAP) family (Labrosse et al., 2005; Colinet et al., 2013).  
85 A LbmGAP ortholog named LbyGAP (previously named LbGAPy) is also present in the venom of the *L.*  
86 *boulardi* ISy line, but in lower amounts (Colinet et al., 2010; Colinet et al., 2013). While RhoGAPs are usually  
87 intracellular proteins composed of several different domains (Tcherkezian & Lamarche-Vane 2007),  
88 LbmGAP and LbyGAP contain only one RhoGAP domain preceded by a signal peptide that allows its  
89 secretion. LbmGAP has been shown to be associated with and transported by venosomes to target host  
90 hemocytes (Wan et al., 2019). LbmGAP and LbyGAP specifically interact with and inactivate two *Drosophila*  
91 Rho GTPases, Rac1 and Rac2 (Colinet et al., 2007; Colinet et al., 2010), which are required for hemocyte  
92 proliferation in response to parasitism, hemocyte adhesion around the parasitoid egg, or the formation of  
93 intercellular junctions necessary for the capsule formation (Williams et al., 2005; Williams et al., 2006).  
94 Combined transcriptomic and proteomic analyses have identified eight additional RhoGAP domain-  
95 containing venom proteins in addition to LbmGAP and LbyGAP for both *L. boulardi* lines, suggesting that a  
96 multigene family has derived from repeated duplication (Colinet et al., 2013). One of these venom

97 RhoGAPs, LbmGAP2 (previously named LbGAP2), has also been shown to be associated with venosomes in  
98 *L. bouleardi* ISm and to be released with LbmGAP in host hemocytes (Wan et al., 2019). Interestingly, three  
99 RhoGAP domain-containing venom proteins have also been identified in the closely related species  
100 *Leptopilina heterotoma* (Colinet et al., 2013), suggesting that the recruitment of RhoGAPs in the venom  
101 arsenal may have occurred before the separation of the two species.

102 *Leptopilina* venom RhoGAPs are not the only example of the possible use of a protein from this family  
103 in parasitoid virulence (Reineke et al., 2006; Du et al., 2020). In the Ichneumonidae *V. canescens*, a RhoGAP  
104 domain-containing protein known as VLP2 (named VcVLP2 in this paper) was found to be associated with  
105 VLPs formed in the nucleus of ovarian calyx cells (Reineke et al., 2006; Pichon et al., 2015). VLPs, which  
106 package proteic virulence factors wrapped into viral envelopes, are then released into the ovarian lumen  
107 to associate with eggs and protect them from the host immune response by as yet unknown mechanisms  
108 (Feddersen et al., 1986). Species of the genus *Leptopilina* (superfamily Cynipoidea) as well as *V. canescens*  
109 (superfamily Ichneumonoidea) belong to the group of parasitoid wasps, which has been shown to be  
110 monophyletic (Peters et al., 2017). They are distantly related, with their last common ancestor dating back  
111 to the early radiation of parasitoid wasps, more than 200 million years ago (Peters et al., 2017). The  
112 presence of RhoGAP family proteins in the maternal fluids of parasitoid wasps has not been described  
113 outside of *Leptopilina* species and *V. canescens*. Overall, these observations suggest convergent  
114 recruitment of proteins belonging to the same family and injected into the host with the egg in two  
115 phylogenetically distant parasitoid species.

116 In this work, we showed that VcVLP2 in *V. canescens*, like LbmGAP in *Leptopilina*, is not unique but is  
117 part of a multigene family of virulent RhoGAPs associated with extracellular vesicles. RhoGAPs from  
118 different organisms are grouped into distinct subfamilies based on similarities in RhoGAP domain sequence  
119 and overall multi-domain organization (Tcherkezian & Lamarche-Vane 2007). Our analyses indicate that an  
120 independent duplication of the RacGAP1 gene, a member of the large RhoGAP family, was the origin of the  
121 two virulent RhoGAP multigene families, one found in *Leptopilina* and the other in *V. canescens*. We then  
122 performed comparative analyses to understand the duplication events at the origin of these two virulent  
123 RhoGAP multigene families. Finally, we demonstrated evolution under positive selection for both virulent  
124 RhoGAP multigene families in *L. bouleardi* and *V. canescens*, suggesting accelerated evolution and functional  
125 diversification.

## 126 **Methods**

### 127 **Biological material**

128 The origin of the *L. bouleardi* isofemale lines ISm (Lbm; Gif stock number 431) and ISy (Lby; Gif stock  
129 number 486) has been described previously (Dupas et al., 1998). Briefly, the ISy and ISm founding females  
130 were collected in Brazzaville (Congo) and Nasrallah (Tunisia), respectively. The *L. heterotoma* strain (Lh; GIF  
131 stock number 548) was collected in southern France (Gotheron). The Japanese strain of  
132 *Leptopilina victoriana* (Lv), described in Novković et al., 2011, was provided by Pr. M. T. Kimura (Hokkaido  
133 University, Japan). All parasitoid lines were reared on a susceptible *D. melanogaster* Nasrallah strain (Gif  
134 stock number 1333) at 25 °C. After emergence, the wasps were maintained at 20 °C on agar medium  
135 supplemented with honey. All experiments were performed on 5- to 10-day-old parasitoid females.

### 136 **Phylogeny of members of the Cynipoidea superfamily**

137 The phylogeny of selected members of the Cynipoidea superfamily was constructed using internal  
138 transcribed spacer 2 (ITS2) sequences available at NCBI (Supplementary Table S1). Multiple sequence  
139 alignment was performed using MAFFT with the --auto option (Katoh & Standley 2013). Poorly aligned  
140 regions were removed using trimal with the -automated1 option (Capella-Gutierrez et al., 2009).  
141 Phylogenetic analysis was performed using maximum likelihood (ML) with IQ-TREE (Minh et al., 2020). [The](#)  
142 [alignments obtained before and after using Trimal are shown in Supplementary Dataset 1.](#)

### 143 **Search for candidate venom RhoGAPs in *Leptopilina* transcriptomes**

144 *L. victoriana* venom apparatus, corresponding to venom glands and associated reservoirs, were  
145 dissected in Ringer's saline (KCl 182 mM; NaCl 46 mM; CaCl<sub>2</sub> 3 mM; Tris-HCl 10 mM). Total RNA was  
146 extracted from 100 venom apparatus using TRIzol reagent (Invitrogen) followed by RNeasy Plus Micro Kit

147 (QIAGEN) according to the manufacturers' instructions. The quality of total RNA was checked using an  
148 Agilent BioAnalyzer. Illumina RNASeq sequencing (HiSeq 2000, 2 × 75 pb) and trimming were performed  
149 by Beckman Coulter Genomics. The raw data are available at NCBI under the BioProject ID PRJNA974978.  
150 Sequence assembly was performed using the "RNASeq de novo assembly and abundance estimation with  
151 Trinity and cdhit" workflow available on Galaxy at the BIPAA platform (<https://bipaa.genouest.org>).

152 *Leptopilina clavipes* (whole body), *Ganaspis* sp. G1 (female abdomen), *Andricus quercuscalicis* (whole  
153 body) and *Synergus umbraculus* (whole body) transcriptomes were obtained from NCBI under accession  
154 numbers GAXY00000000, GAIW00000000, GBNY00000000 and GBWA00000000, respectively. Coding  
155 regions in the transcripts were identified and translated using TransDecoder (Haas et al., 2013), which is  
156 available on the BIPAA Galaxy platform. Searches for RhoGAP domain-containing sequences in translated  
157 coding sequences were performed using hmmsearch from the HMMER package (Eddy 2009) with the  
158 RhoGAP (PF00620) HMM profile.

### 159 **Completion of *L. bouleari* and *L. heterotoma* venom RhoGAP sequences**

160 Venom apparatus, corresponding to venom glands and associated reservoirs, were dissected in Ringer's  
161 saline. Total RNA was extracted from venom apparatus using the RNeasy Plus Micro Kit (QIAGEN) according  
162 to the manufacturers' instructions. To obtain the full-length coding sequence of LbmGAP1.3, LbmGAP5,  
163 LbyGAP6, LhGAP1 and LhGAP2, rapid amplification of cDNA ends (RACE) was performed using the SMART  
164 RACE cDNA Amplification Kit (Clontech). For LhGAP3, 3' RACE could not be applied due to the presence of  
165 poly(A) stretches in the sequence. LhGAP3-matching sequences were searched for in the transcriptome  
166 assembly obtained by Goecks et al., 2013) from the abdomen of *L. heterotoma* females (GenBank accession  
167 number GAJC00000000) using the command line NCBI-BLAST package (version 2.2.24). The resulting  
168 complete LhGAP3 sequence was then verified by RT-PCR using the iScript cDNA Synthesis Kit (BioRad) and  
169 the GoTaq DNA Polymerase (Promega), followed by direct sequencing of the amplified fragment. Geneious  
170 software (Biomatters) was used for sequence editing and assembly.

### 171 **Obtention of *Leptopilina* RacGAP1 coding sequences**

172 A combination of RT-PCR and RACE using conserved and specific primers was used to clone the full-  
173 length ORF sequence of *L. bouleari* ISm and *L. heterotoma* RacGAP1. The amino acid sequence of *Nasonia*  
174 *vitripennis* RacGAP1 (Supplementary Table S2) was used to search for similar sequences among  
175 Hymenoptera species using BLASTP at NCBI (<http://www.ncbi.nlm.nih.gov/blast/>). A multiple sequence  
176 alignment of the RacGAP1 amino acid sequences found in Hymenoptera was then performed using  
177 MUSCLE (Edgar 2004). Two pairs of RacGAP1-specific degenerate primers were designed from the  
178 identified conserved regions (Supplementary Figure S1). Total RNA was extracted from Lbm and Lh  
179 individuals using the TRIzol reagent (Invitrogen), and RT-PCR experiments were performed using the  
180 RacGAP1-specific degenerate primers. After direct sequencing of the amplified fragments, Lbm- and Lh-  
181 specific primers were designed to complete the sequences obtained by RT-PCR and RACE (Supplementary  
182 Figure S1). The coding sequences of ~~*L. victoriae*~~ and ~~*L. clavipes*~~ RacGAP1 ~~were~~ obtained by BLAST  
183 searches in the corresponding transcriptomes using *L. bouleari* ISm and *L. heterotoma* RacGAP1 sequences  
184 as queries.

### 185 **Obtention of the genomic sequences of *Leptopilina* venom RhoGAPs and RacGAP1**

186 The genomic sequences of *Leptopilina* venom RhoGAPs and RacGAP1 were obtained by BLAST and  
187 Exonerate searches (Slater & Birney 2005) using the corresponding coding sequences as queries. *L. bouleari*  
188 ISm, *L. bouleari* ISy, *L. heterotoma* and *L. clavipes* genome assemblies were obtained from NCBI under  
189 accession numbers GCA\_011634795.1, GCA\_019393585.1, GCF\_015476425.1 and GCA\_001855655.1  
190 respectively.

### 191 **Search for candidate *V. canescens* RhoGAP calyx sequences**

192 Coding regions were identified from the *V. canescens* calyx transcriptome published by Pichon et al.,  
193 (2015) and translated into protein sequences using TransDecoder (Haas et al., 2013). The search for  
194 RhoGAP domain-containing sequences was performed using hmmsearch from the HMMER package (Eddy  
195 2009) with the RhoGAP (PF00620) HMM profile. The identified RhoGAP calyx sequences were used as a

196 database for Mascot to explore MS/MS data obtained from purified *V. canescens* VLPs (Pichon et al., 2015)  
197 with a false discovery rate of 1%. Only proteins identified by two or more peptides were considered.

198 The *V. Canescens* RacGAP1 coding sequence was obtained by BLAST searches in the *V. canescens* calyx  
199 transcriptome using the *N. vitripennis* RacGAP1 sequence as query.

200 The *V. canescens* calyx RhoGAP and RacGAP1 genome sequences were obtained by BLAST and  
201 Exonerate searches (Slater and Birney 2005) using the corresponding coding sequences as queries. The *V.*  
202 *canescens* genome assembly was obtained from NCBI under accession number GCA\_019457755.1.

### 203 Identification of domains and motifs and prediction of subcellular localization

204 The presence and position of signal peptide cleavage sites in the identified RhoGAP domain-containing  
205 sequences were predicted using the SignalP server  
206 (<https://services.healthtech.dtu.dk/service.php?SignalP>). The searches for domains and motifs were  
207 performed using InterProScan 5 (Jones et al., 2014) on the InterPro integrative protein signature database  
208 (<https://www.ebi.ac.uk/interpro/>). Coiled-coil regions were predicted using COILS (Lucas et al., 1991).

209 To identify the possible origin of the signal peptide of *Leptopilina* venom RhoGAPs, we performed a  
210 similarity search using Exonerate (Slater and Birney 2005) with the exon(s) preceding the RhoGAP domain  
211 in the genomes of *L. bouvardi* ISm and ISy, *L. clavipes* and *L. heterotoma*.

212 Prediction of protein subcellular localization and sorting signals for *Venturia* RacGAP1 and calyx  
213 RhoGAPs was performed using the DeepLoc2 server ([https://services.healthtech.dtu.dk/services/DeepLoc-](https://services.healthtech.dtu.dk/services/DeepLoc-2.0/)  
214 [2.0/](https://services.healthtech.dtu.dk/services/DeepLoc-2.0/)).

215 Nuclear localization for VcRacGAP1 and calyx RhoGAPs was also predicted using the following three  
216 tools: NucPred (Brameier et al., 2007) was used to indicate whether a protein spends part of its time in the  
217 nucleus (<https://nucpred.bioinfo.se/nucpred/>), LocTree3 (Goldberg et al., 2014) to provide subcellular  
218 localization and Gene Ontology terms (<https://roslab.org/services/loctree3/>), and PSORT II (Nakai &  
219 Horton 1999) to detect sorting signals and subcellular localization (<https://psort.hgc.jp/form2.html>).  
220 PSORT II results corresponding to ER membrane retention signals and cleavage sites for mitochondrial  
221 presequences were included as they may be associated with nuclear localization. Mitochondrial  
222 presequences have no sequence homology but possess physical characteristics that allow them to interact  
223 with the outer membranes of mitochondria and thus allow the targeting of proteins to the mitochondrial  
224 matrix. Regarding mitochondrial targeting, it has been shown from plants to humans that some proteins  
225 with mitochondrial presequences are dually targeted to mitochondria and the nucleus (Millar et al., 2006;  
226 Mueller et al., 2004). Indeed, anchoring signals to the ER membrane are known to allow baculoviral  
227 proteins to migrate to the inner nuclear membrane (Braunagel et al., 1996). Proteins forming VLPs in *V.*  
228 *canescens* could thus follow the same pathways as their homologous proteins in baculoviruses, nudiviruses,  
229 hytrosaviruses, and bracoviruses due to the conservation of this mechanism among these viruses belonging  
230 to the order Lefavirales (Braunagel et al., 1996; Hong et al., 1997; Braunagel et al., 2004; Abd-Alla et al.,  
231 2008; Bézier et al., 2009; Braunagel et al., 2009).

### 232 Phylogeny of *Leptopilina* venom and *Venturia* calyx RhoGAPs

233 Searches for *N. vitripennis* RhoGAP sequences were performed using BLASTP at NCBI  
234 (<http://www.ncbi.nlm.nih.gov/blast/>) and hmmsearch from the HMMER package (Eddy 2009) with the  
235 RhoGAP (PF00620) HMM profile on the *N. vitripennis* v2 proteome database (Rago et al., 2016).

236 For the phylogenetic analysis of *Leptopilina* venom and *Venturia* calyx RhoGAPs, multiple alignments  
237 of the RhoGAP domain amino acid sequences were performed using MAFFT with the --auto option (Kato  
238 and Standley 2013). For codon-based analysis of selection (see below), codon-based alignments of  
239 complete coding sequences were performed using RevTrans  
240 (<https://services.healthtech.dtu.dk/service.php?RevTrans>) with the amino acid alignments as templates.  
241 Poorly aligned regions were removed using trimAl with the -automated1 option (Capella-Gutierrez et al.,  
242 2009). Phylogenetic analyses were performed using maximum likelihood (ML) with IQ-TREE (Minh et al.,  
243 2020). ModelFinder was used to select the best model selection for phylogeny (Kalyaanamoorthy et al.,  
244 2017). The alignments obtained before and after using Trimal are shown in Supplementary Dataset 1.

### 245 Codon-based analysis of selection

246 Codon-based alignments of complete coding sequences were performed with RevTrans using the  
247 amino acid alignments as templates (see above). Phylogenetic analyses were performed using maximum  
248 likelihood (ML) with PhyML (Guindon et al., 2010). Smart Model Selection was used to choose the best  
249 model selection for the phylogeny (Lefort et al., 2017).

250 To detect evolutionary selective pressures acting on RhoGAP sequences, the ratios of non-synonymous  
251 substitutions (dN) to synonymous substitutions (dS) were compared using different ML frameworks: the  
252 CODEML program in the PAML (Phylogenetic Analysis by Maximum Likelihood) package (Yang 1997; Yang  
253 2007), the HyPhy software implemented at <http://www.datamonkey.org/> (Delpont et al., 2010), and the  
254 Selecton server (Stern et al., 2007) available at <http://selecton.tau.ac.il/index.html>.

255 Five different methods were used to detect codons under positive selection. In the first, codon  
256 substitution models implemented in CodeML were applied to the codon-based alignment using the F3x4  
257 frequency model. Two pairs of site models were used to determine whether some codons were under  
258 positive selection: M1a (neutral) versus M2a (selection) and M7 (beta distribution where  $0 < \omega$  (dN/dS  
259 ratio)  $< 1$ ) versus M8 (beta distribution as in M7 with  $\omega > 1$  as additional class). The models were compared  
260 using a likelihood ratio test (LRT) with 2 degrees of freedom to assess the significance of detection of  
261 selection (Yang et al., 2000). Bayes Empirical Bayes (BEB) inference was then used to identify amino acid  
262 sites with a posterior probability  $>95\%$  of being under positive selection (Yang et al., 2005). We then applied  
263 four other methods of detection of selection available in the HyPhy package: Single Likelihood Ancestor  
264 Counting (SLAC), Fixed Effect Likelihood (FEL), Mixed Effects Model of Evolution (MEME) and Fast Unbiased  
265 Bayesian AppRoximation (FUBAR) methods (Kosakovsky Pond & Frost 2005; Murrell et al., 2012; Murrell et  
266 al., 2013). To eliminate false-positive detection, only codons identified by CodeML M2a and M8 and at least  
267 one of the other methods were considered under positive selection. Radical or conservative replacements  
268 were then determined based on whether they involved a change in the physicochemical properties of a  
269 given amino acid, such as charge or polarity (Zhang 2000).

270 Four different methods were used to detect codons under negative selection: the Selecton server using  
271 the pair of site models M8a ( $\beta$  &  $\omega=1$ ) versus M8 ( $\beta$  &  $\omega$ ), and the FEL, SLAC and FUBAR methods mentioned  
272 above. Only codons identified by Selecton and at least one other method were considered under purifying  
273 selection.

274 To identify specific lineages with a proportion of sites evolving under positive or purifying selection, we  
275 performed branch-site REL analyses using the HyPhy package (Kosakovsky Pond et al., 2011). Unlike the  
276 branch and branch-site lineage-specific models available in CodeML, branch-site REL does not require *a*  
277 *priori* identification of foreground and background branches.

## 278 **Structural analysis**

279 Molecular modeling of VcVLP2 RhoGAP was performed using the Phyre server with default parameters  
280 (<http://www.sbg.bio.ic.ac.uk/phyre2/>) (Kelley et al., 2015). The model with the highest confidence (100%)  
281 and coverage (46%) was obtained using the crystal structure with PDB code 2OVJ as a template. Model  
282 quality was evaluated using the QMEAN server (<http://swissmodel.expasy.org/qmean/>) (Benkert et al.,  
283 2011). Briefly, the QMEAN score is a global reliability score with values ranging between 0 (lower accuracy)  
284 and 1 (higher accuracy). The associated Z-score relates this QMEAN score to the scores of a non-redundant  
285 set of high-resolution X-ray structures of similar size, with ideal values close to 0. Visualization of LbmGAP  
286 (Colinet et al., 2007) and VcVLP2 structures and mapping of sites under selection were performed using  
287 PyMol (<http://sourceforge.net/projects/pymol/>). Secondary structure assignment was performed with the  
288 DSSP program (Kabsch & Sander 1983). Accessible surface area (ASA) or solvent accessibility of amino acids  
289 was predicted using the ASAView algorithm (Ahmad et al., 2004).

## 290 **In vitro mutagenesis**

291 The S76K, V124K, L137D, T143L, S150L, I185K, E200G, and V203R mutations were introduced into the  
292 LbmGAP cDNA using the QuickChange XL Site-Directed Mutagenesis Kit (Stratagene). The results of *in vitro*  
293 mutagenesis were verified by sequencing.

## 294 **Yeast two-hybrid analysis**

295 Interactions between LbmGAP and LbmGAP mutants and mutated forms of *Drosophila* RhoA, Rac1,  
296 Rac2 and Cdc42 GTPases were individually examined by mating as previously described (Colinet et al.,

297 2007). The plasmids expressing the GTPase proteins were tested against the pGADT7-T control vector,  
298 which encodes a fusion between the GAL4 activation domain and the SV40 large T-antigen. Reciprocally,  
299 plasmids producing LbmGAP and LbmGAP mutants were tested against the pLex-Lamin control vector.  
300 Interactions between LbmGAP and the Rac1 and Rac2 GTPases were used as positive controls (Colinet et  
301 al., 2007). Interactions were initially tested by spotting five-fold serial dilutions of cells on minimal medium  
302 lacking histidine and supplemented with 3-amino-triazole at 0.5 mM to reduce the number of false  
303 positives.  $\beta$ -galactosidase activity was then detected on plates (Fromont-Racine et al., 1997).

#### 304 **Purification of *Leptopilina* venosomes and mass spectrometry analysis**

305 Twenty-five Lbm, Lby and Lh female venom apparatus were dissected and the reservoirs separated  
306 from the gland. The twenty-five reservoirs were then pooled and opened to release the venom content in  
307 25  $\mu$ l of Ringer's solution supplemented with a protease inhibitor cocktail (Sigma). The venom suspension  
308 was centrifuged at 500xg for 5 min to remove the residual tissues, then centrifuged at 15,000xg for 10 min  
309 to separate the vesicular fraction from the soluble venom proteins (supernatant fraction) (Wan et al.,  
310 2019). The vesicular fraction was then washed twice by resuspension in 25  $\mu$ l of Ringer's solution followed  
311 by centrifugation at 15,000xg for 10 min. The two samples were mixed with 4x Laemmli buffer containing  
312  $\beta$ -mercaptoethanol (v/v) and boiled for 5 min. Proteins were then separated on a 6–16% linear gradient  
313 SDS-PAGE and the gel was silver stained as previously described (Colinet et al., 2013). Identification of  
314 proteins by nano-LC-tandem mass spectrometry (MS/MS) was performed on bands excised from the gels  
315 as previously described (Colinet et al., 2013). MS/MS data analysis was performed with Mascot software  
316 (<http://www.matrixscience.com>), licensed in house using the full-length coding sequences of the  
317 *Leptopilina* venom RhoGAP sequences. Data validation criteria were (i) one peptide with individual ion  
318 score greater than 50 or (ii) at least two peptides of individual ion score greater than 20. The mascot score  
319 is calculated as  $-10\log(p)$ . The number of peptide matches identified by Mascot software on the MS/MS  
320 data was used to determine (i) the number of protein bands in which each venom RhoGAP was found and  
321 (ii) the protein band in which each venom RhoGAP was the most abundant. The calculated FDR (based on  
322 an automated decoy database search) was less than 1%. The mass spectrometry proteomics data have  
323 been deposited to the ProteomeXchange Consortium via the PRIDE (Perez-Riverol et al., 2022) partner  
324 repository with the dataset identifier PXD041695.

## 325 **Results**

### 326 ***Leptopilina* venom RhoGAPs probably emerged in the ancestor of the genus**

327 In the Figitidae, venom RhoGAPs have only been described for *L. bouleardi* and *L. heterotoma* (Labrosse  
328 et al., 2005; Colinet et al., 2013). A search for candidate homologs was performed in the transcriptomes of  
329 *L. victoriae* and *L. clavipes*, two other *Leptopilina* species, *Gasnaspis* sp. G1, another member of the family  
330 Figitidae, and *Andricus quercuscalicis* and *Synergus umbraculus*, two gall wasp species representatives of  
331 the superfamily Cynipoidea outside of Figitidae (separated by approximately 50 Mya (Peters et al., 2017)).  
332 The putative venom RhoGAPs were identified based on the presence of a signal peptide at the N-terminus  
333 of the protein, followed by a RhoGAP domain (Table 1). Two transcript sequences encoding RhoGAP  
334 domain-containing proteins predicted to be secreted were found in *L. victoriae* (LvGAP1 and LvGAP2) and  
335 one in *L. clavipes* (LcGAP1), whereas none were found for *Gasnaspis* sp. G1, *A. quercuscalicis* and *S.*  
336 *umbraculus* (Table 1 and Figure 1A). Our results therefore suggest that venom RhoGAPs are specific to the  
337 genus *Leptopilina* although further taxon sampling would be required to fully support this hypothesis.

### 338 ***Leptopilina* venom RhoGAPs likely evolved from a single imperfect duplication of RacGAP1**

339 A phylogenetic analysis was performed to learn more about the evolutionary history of *Leptopilina*  
340 venom RhoGAPs. The phylogeny was constructed based on the amino acid sequence of the RhoGAP  
341 domain of these venom proteins and that of the 19 RhoGAPs we identified from the predicted proteome  
342 of the jewel wasp *Nasonia vitripennis* (Supplementary Table S2). *N. vitripennis* (superfamily Chalcidoidea)  
343 was chosen because it was the first parasitoid wasp to have its genome sequenced, and its genome has  
344 recently been re-annotated (Rago et al., 2016). Furthermore, the only RhoGAPs found in *N. vitripennis* are  
345 classical intracellular RhoGAPs, which are absent in maternal fluids (de Graaf et al., 2010).

346 Prior to phylogenetic analysis, the complete coding sequence was obtained for two Lbm (LbmGAP1.3  
 347 and LbmGAP5), one Lby (LbyGAP6) and all three Lh venom RhoGAPs as described in the Methods section.  
 348 Two of the *Leptopilina* venom RhoGAPs, namely LhGAP3 and LcGAP1, were predicted to contain two  
 349 RhoGAP domains instead of one. Therefore, these two domains were separated for the analysis. The  
 350 resulting phylogeny identified NvRacGAP1 as the closest RhoGAP from *N. vitripennis* to all *Leptopilina*  
 351 venom RhoGAPs with confident support values (Figure 1B). Accordingly, the RhoGAP domain found in all  
 352 *Leptopilina* venom RhoGAPs was predicted to belong to the RacGAP1 subfamily typically found in RacGAP1-  
 353 related proteins (Table 1). These results suggest that the *Leptopilina* venom RhoGAPs derive from  
 354 duplication of the *N. vitripennis* RacGAP1 ortholog in *Leptopilina*.

355 **Table 1.** Motif and domain organization of *Leptopilina* venom RhoGAPs. The signal peptide was  
 356 predicted using SignalP at CBS. The RhoGAP domain (PF00620) from the Pfam database and the  
 357 RacGAP1 domain (PTHR46199) from the Panther database were identified using InterProScan on the  
 358 InterPro integrative protein signature database. Compared to Pfam, the Panther database provides  
 359 information about the specific RhoGAP subfamily to which the domain belongs. Two successive  
 360 RhoGAP domains were found in LhGAP3 and LcGAP1. Lbm: *L. bouleardi* ISm ; Lby: *L. bouleardi* ISy ; Lh:  
 361 *L. heterotoma* ; Lc: *L. clavipes* ; Lv: *L. victoricae*. The dot numbering (e.g., LbmGAP1.1, LbmGAP1.2, and  
 362 LbmGAP1.3) was used for *Leptopilina* venom RhoGAPs that are encoded by different genes but share  
 363 high amino acid sequence identity in the RhoGAP domain (greater than 70% identity).

		Total length	Signal peptide		RhoGAP domain (PF00620)				RacGAP1 domain (PTHR46199)			
			From	To	From	To	Length	E-value	From	To	Length	E-value
Lbm	LbmGAP	282	1	20	52	193	142	2.9e-32	38	267	230	7.0e-37
	LbmGAP1.1	292	1	23	58	205	148	1.0e-19	42	255	214	7.0e-30
	LbmGAP1.2	280	1	23	58	205	148	1.1e-19	42	255	214	1.3e-29
	LbmGAP1.3	287	1	23	58	205	148	7.2e-17	42	253	212	1.3e-27
	LbmGAP2.1	251	1	23	44	183	140	9.9e-26	26	234	209	5.5e-37
	LbmGAP2.2	263	1	23	56	196	141	6.6e-26	49	246	198	1.3e-34
	LbmGAP3	295	1	23	56	175	120	3.2e-12	42	266	225	1.2e-27
	LbmGAP4	246	1	20	42	178	137	9.1e-11	38	218	181	5.6e-18
	LbmGAP5	275	1	20	60	207	148	6.3e-23	41	251	211	2.4e-33
Lby	LbyGAP	286	1	20	52	193	142	1.6e-32	38	267	230	3.4e-37
	LbyGAP1.1	287	1	23	58	205	148	5.6e-17	42	255	214	9.9e-28
	LbyGAP1.2	325	1	23	56	203	148	2.9e-17	42	293	252	1.7e-26
	LbyGAP2	256	1	23	44	185	142	8.3e-27	26	234	209	1.5e-37
	LbyGAP3.1	281	1	23	56	175	120	1.8e-11	42	237	196	1.5e-25
	LbyGAP3.2	266	1	23	41	160	120	5.8e-12	28	222	195	6.4e-25
	LbyGAP4	274	1	20	42	177	136	7.4e-09	30	218	189	2.1e-17
	LbyGAP5	275	1	23	60	207	148	4.4e-24	41	251	211	1.2e-35
LbyGAP6	239	1	20	53	194	142	8.2e-25	49	231	183	9.4e-34	
Lh	LhGAP1	293	1	20	43	180	138	5.5e-36	41	289	249	1.0e-38
	LhGAP2	336	1	20	43	181	139	1.5e-29	45	275	231	8.2e-31
	LhGAP3	467	1	20	35	174	140	1.4e-22	34	221	188	1.3e-38
Lc	LcGAP1	497	1	20	257	396	140	2.2e-17	247	478	232	8.46e-71
					43	184	142	3.2e-30				
Lv	LvGAP1	370	1	20	38	179	142	2.4e-30	33	224	192	3.7e-28
	LvGAP2	266	1	20	38	181	144	8.5e-23				

364  
 365  
 366 The RacGAP1 coding sequence of *L. bouleardi* ISm, *L. heterotoma*, ~~*L. victoricae*~~ and *L. clavipes* was  
 367 obtained either by cloning and sequencing or by searching genomic data, and its domain organization was  
 368 compared with that of venom RhoGAPs (Figure 1C, Table 1 and Supplementary Figure S2). *Leptopilina*  
 369 RacGAP1 has a typical domain organization consisting of a coiled-coil region and a C1 motif (protein kinase



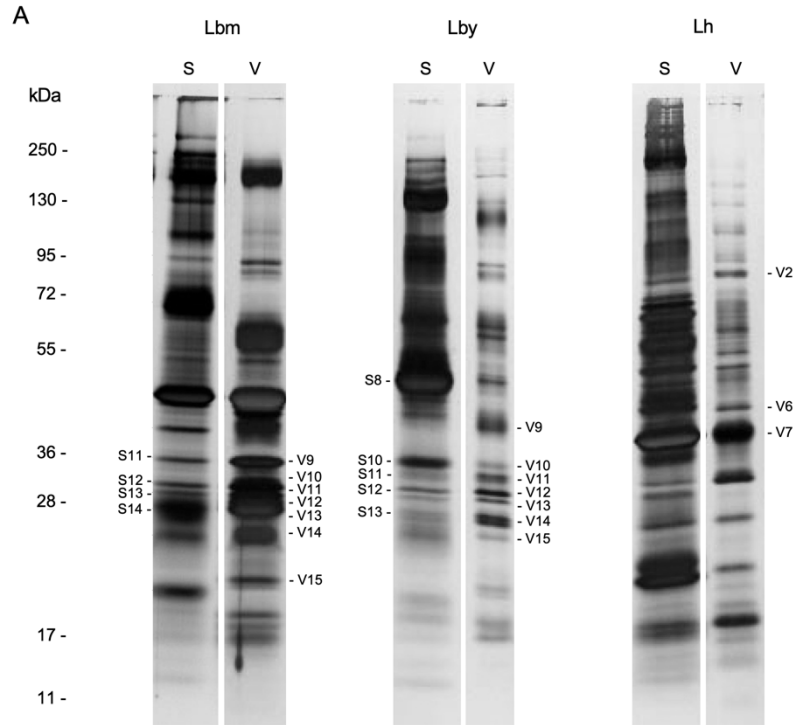


382 *Synergus umbraculus*. The scale bar indicates the number of substitutions per site. (B) Maximum-  
383 likelihood phylogenetic tree of *Leptopilina* venom RhoGAPs along with *N. vitripennis* classical  
384 RhoGAPs. (C) Comparison of protein domain organization between LbmGAP, representative of most  
385 *Leptopilina* venom RhoGAPs, LhGAP3 and LcGAP1, the two venom RhoGAPs that contain two RhoGAP  
386 domains, and *Leptopilina* RacGAP1. (D) Maximum-likelihood phylogenetic tree of *Venturia* calyx  
387 RhoGAPs along with *N. vitripennis* classical RhoGAPs. (E) Comparison of protein domain organization  
388 between VcGAP1, VcVLP2 and VcGAP12, representative of the other *Venturia* calyx RhoGAPs, and  
389 *Venturia* RacGAP1. In A, B, and D, numbers at corresponding nodes are bootstrap support values in  
390 percent (500 bootstrap replicates). Only bootstrap values greater than 70% are shown. In B and D,  
391 the phylogenetic tree was obtained with IQ-TREE using the RhoGAP domain amino acid sequence and  
392 displayed as a cladogram. *Leptopilina* venom RhoGAPs and *Venturia* calyx RhoGAPs are highlighted  
393 in blue. The tree was rooted at midpoint. In C and E, C1: protein kinase C-like zinc finger motif, CC:  
394 coiled-coil region, RhoGAP: RhoGAP domain found in RacGAP1-related proteins, SP: signal peptide.

395 To further investigate this duplication event and the possible origin of the signal peptide, the genomic  
396 sequences of *L. bouleardi* ISm, *L. heterotoma* and *L. clavipes* venom RhoGAPs and RacGAP1 were obtained,  
397 either by cloning and sequencing or by searching in genomic data, and compared (Supplementary Table  
398 S3). The genomic sequence of *Leptopilina* RacGAP1 consists of 10 exons with a “CC region”, “C1 motif” and  
399 “RhoGAP domain” encoded by exons 2 and 3, exons 5 and 6 and exons 7 and 8, respectively. The RhoGAP  
400 domain is also encoded by two exons for venom RhoGAPs. These two exons are preceded by one to three  
401 exons, with the signal peptide encoded by the first exon for most of them. Sequence comparisons revealed  
402 similarities between venom RhoGAPs and *Leptopilina* RacGAP1 only for the sequence spanning the two  
403 exons encoding the RhoGAP domain and part of the following one. No significant similarities were found  
404 for the preceding exons at either the nucleotide or amino acid level (Supplementary Figure S3). This  
405 supports the hypothesis of a partial duplication of the RacGAP1 gene in the ancestor of the *Leptopilina*  
406 genus, resulting in the loss of the sequence spanning exons 1 to 6, followed by further duplication of the  
407 ancestrally duplicated gene during the diversification of the genus *Leptopilina*. No significant sequence  
408 similarity was found between the exon(s) preceding the RhoGAP domain coding sequence of *Leptopilina*  
409 venom RhoGAPs and other sequences in the genomes of *L. bouleardi* ISm and ISy, *L. clavipes*, and *L.*  
410 *heterotoma* that could provide an indication of the origin of the signal peptide (Supplementary Dataset 2).  
411 Some of the duplication events that followed the initial duplication of the RacGAP1 gene in the ancestor  
412 of the *Leptopilina* genus appear to be specific to *L. bouleardi* and would explain the large number of venom  
413 RhoGAPs found in this species (Figure 1B and Supplementary Figure S2). The two consecutive RhoGAP  
414 domains found in LhGAP3 were grouped together with confident support values in the phylogenies (Figure  
415 1B and Supplementary Figure S2). This suggests that a partial tandem duplication spanning exons 2 and 3  
416 has occurred for this *L. heterotoma* venom RhoGAP. In contrast, the two RhoGAP domains found in LcGAP1  
417 did not group together (Figure 1B and Supplementary Figure S2). However, the genomic sequence of  
418 LcGAP1 was not complete and we could not find the region corresponding to the second RhoGAP domain  
419 in the *L. clavipes* genome (Supplementary Table S3). Therefore, it is unclear whether the LcGAP1 coding  
420 sequence found in the transcriptome assembly is true or artifactual.

#### 421 ***L. bouleardi* and *L. heterotoma* venom RhoGAPs are associated with venosomes**

422 LbmGAP and LbmGAP2 have been shown to be associated with vesicles named venosomes produced  
423 in *L. bouleardi* venom that transport them to *Drosophila* lamellocytes (Wan et al., 2019). Our next goal was  
424 to investigate whether *Leptopilina* venom RhoGAPs other than LbmGAP and LbmGAP2 could be associated  
425 with venosomes. Proteomic analysis was performed on the supernatant and vesicular fractions separated  
426 from the venom by centrifugation. Comparison of the electrophoretic profiles obtained on a 6-16% SDS-  
427 PAGE for *L. bouleardi* ISm (Lbm), *L. bouleardi* ISy (Lby) and *L. heterotoma* (Lh) revealed an important variation  
428 between both fractions for all three wasps (Figure 2). All the major bands on the electrophoretic patterns  
429 of Lbm, Lby and Lh supernatant and vesicular fractions, as well as several minor bands (35 bands in total  
430 for Lbm, 34 for Lby and 37 for Lh), were excised and tryptic peptides were analyzed by mass spectrometry.  
431 The coding sequences of *Leptopilina* venom RhoGAPs were used to perform Mascot searches on the mass  
432 spectrometry data obtained from both venom fractions. All *L. bouleardi* and *L. heterotoma* venom RhoGAPs  
433 were detected in the vesicular fraction, where most of them were found to be enriched (Figure 2). We  
434 could then hypothesize that they are associated with and transported by venosomes to target *Drosophila*  
435 cells.



**B**

		Length	Predicted Mw	Supernatant		Vesicular	
				Protein band	Mascot Matches	Protein band	Mascot Matches
Lbm	LbmGAP	282	32.13	<b>S11/S12</b>	11	<b>V9/V10/V11/V12/V13/V14/V15</b>	57
	LbmGAP1.1	292	33.02	S11/ <b>S12</b> /S14	14	V9/ <b>V10</b> /V11/V12/V14/V15	85
	LbmGAP1.2	280	31.99	S13	3	<b>V10/V11/V12/V13</b>	36
	LbmGAP1.3	287	32.80	S12/ <b>S13</b> /S14	12	V9/V10/ <b>V11</b> /V12/V13/V14/V15	85
	LbmGAP2.1	251	28.81	S11/S12/S13/ <b>S14</b>	14	V10/V11/V12/ <b>V13</b> /V14/V15	60
	LbmGAP2.2	263	30.18	S12/S13/ <b>S14</b>	9	V9/V10/V11/ <b>V12</b> /V13/V14/V15	85
	LbmGAP3	295	34.01	<b>S12</b> /S13	3	<b>V10/V11/V12/V13</b>	15
	LbmGAP4	246	28.57			<b>V13/V14</b>	3
	LbmGAP5	275	31.72			<b>V10/V11</b>	10
	LbyGAP	286	32.56	<b>S8</b>	1	<b>V10/V11</b>	4
Lby	LbyGAP1.1	287	32.81	S10/S11/ <b>S12</b> /S13	19	V11/ <b>V12</b> /V13	19
	LbyGAP1.2	325	37.47			<b>V13</b>	1
	LbyGAP2	256	29.37	<b>S8</b> /S13	8	V12/V13/ <b>V14</b>	8
	LbyGAP3.1	281	32.58	<b>S11</b>	1	V10/ <b>V11</b> /V12/V13	5
	LbyGAP3.2	266	30.74	<b>S11</b>	1	V10/ <b>V11</b> /V12/V13	5
	LbyGAP4	274	31.92	S10/ <b>S11</b> /S12/S13	9	V9/V10/ <b>V11</b> /V12/V13/V14/V15	36
	LbyGAP5	275	32.04			<b>V12</b>	1
	LbyGAP6	239	27.83			<b>V15</b>	3
Lh	LhGAP1	293	33.16			<b>V7</b>	13
	LhGAP2	336	38.23			<b>V6</b>	4
	LhGAP3	467	53.92			<b>V2</b>	7

436

437  
438  
439  
440  
441  
442  
443  
444  
445  
446

**Figure 2. Proteomic analysis of *Leptopilina* venom supernatant and vesicular fractions.** (A) The supernatant (S) and vesicular (V) fractions obtained from 25 Lbm, Lby and Lh venom reservoirs were separated on a 6-16% SDS-PAGE under reducing conditions and visualized by silver staining. Protein bands in which *Leptopilina* venom RhoGAPs were identified by mass spectrometry are numbered on the gel. Molecular weight standard positions are indicated on the left (kDa). (B) For each *Leptopilina* venom RhoGAP, length (number of amino acids), predicted Mw (kDa), bands in which specific peptides were found by mass spectrometry and number of total Mascot matches [using the coding sequences of \*Leptopilina\* venom RhoGAPs as database and](#) according to the S and V venom fractions are given. Numbers in bold correspond to the bands in which each RhoGAP was identified as the most abundant according to the number of Mascot matches.

447 **V. canescens calyx RhoGAPs probably evolved from two or more imperfect RacGAP1 duplication events**

448 Analysis of the *V. canescens* calyx transcriptome allowed the identification of a total of 13 RhoGAP  
 449 domain-containing protein coding sequences, including VcVLP2 (Table 2 and Supplementary Table S4).  
 450 Matches with peptides obtained from a proteomic analysis of *V. canescens* VLPs (Pichon et al., 2015) were  
 451 detected for all 13 calyx RhoGAPs, indicating that they are associated with VLPs (Table 2).

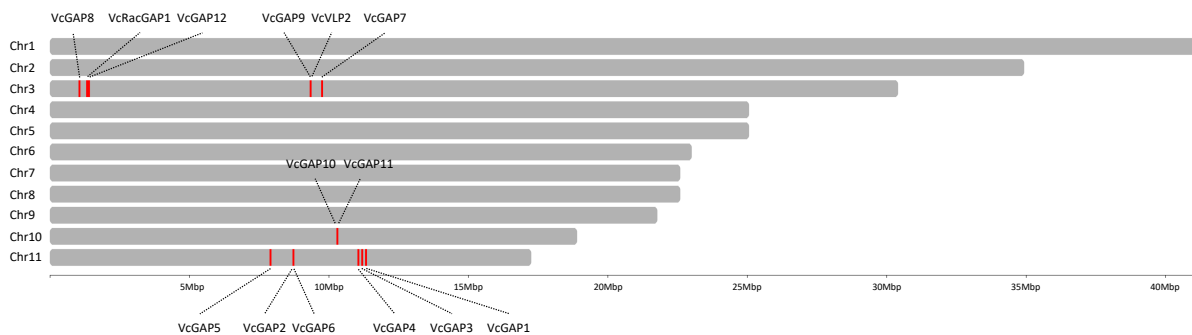
452 Similar to the *Leptopilina* venom RhoGAPs, the *V. canescens* calyx RhoGAPs contain a RacGAP1 domain  
 453 (Table 2) and are closely related to NvRacGAP1 (Figure 1D). A phylogenetic analysis was performed on  
 454 *Leptopilina* venom RhoGAPs and *V. canescens* calyx RhoGAPs, together with *Leptopilina* and *V. canescens*  
 455 RacGAP1 and *N. vitripennis* classical RhoGAPs, using either protein- or codon-based alignment of the  
 456 RhoGAP domain (Supplementary Figure S4). The analysis confirmed a relationship between either  
 457 *Leptopilina* venom RhoGAPs or *V. canescens* calyx RhoGAPs with RacGAP1. In the codon-based phylogeny,  
 458 *V. canescens* calyx RhoGAPs formed a robust monophyletic group with VcRacGAP1, suggesting an  
 459 independent duplication event (Supplementary Figure S4). However, in the protein-based phylogeny, the  
 460 *V. canescens* calyx RhoGAPs did not form a robust monophyletic group with VcRacGAP1. Similarly, the  
 461 *Leptopilina* venom RhoGAPs did not group with *Leptopilina* RacGAP1 in either phylogeny. This is likely due  
 462 to the high divergence of *Leptopilina* venom RhoGAPs and *V. canescens* calyx RhoGAPs compared to  
 463 RacGAP1 (Supplementary Figure S4).

464 In contrast to the *Leptopilina* venom RhoGAPs, none of the *V. canescens* calyx proteins were predicted  
 465 to be secreted. Most were predicted to be localized in the nucleus and/or to contain a nuclear localization  
 466 signal (Supplementary Tables S5 and S6). The absence of a predicted nuclear localization signal for VcGAP7  
 467 may be explained by the incomplete coding sequence at the 5' end (Table 2). There is greater variation in  
 468 domain organization for *V. canescens* calyx RhoGAPs compared to *Leptopilina* venom RhoGAPs (Figure 1E  
 469 and Supplementary Figure S54). Eight *V. canescens* calyx RhoGAPs have retained the C1 motif. In addition,  
 470 VcGAP12 still contains a CC region in the N-terminal part of the sequence although the total sequence  
 471 length is shorter than RacGAP1 (Figure 1E and Supplementary Figure S54).

472 **Table 2.** Motif and domain organization of *Venturia* calyx RhoGAP proteins associated with VLPs. The  
 473 coiled-coil (CC) region was predicted using COILS (Lucas et al., 1991). The protein kinase C-like zinc  
 474 finger (C1) motif (PS50081) from the Prosite database, the RhoGAP domain (PF00620) from the Pfam  
 475 database and the RacGAP1 domain (PTHR46199) from the Panther database were identified using  
 476 InterProScan on the InterPro integrative protein signature database. Compared to Pfam, the Panther  
 477 database provides information about the specific RhoGAP subfamily to which the domain belongs.  
 478 Mascot: number of matches with peptides from purified *V. canescens* VLPs. <sup>a</sup>Coding sequence not  
 479 complete at 5' end. <sup>b</sup>Coding sequence not complete at 3' end.

	Mascot	Total length	CC		C1 (PS50081)		RhoGAP domain (PF00620)				RacGAP1 domain (PTHR46199)			
			From	To	From	To	From	To	Length	E-value	From	To	Length	E-value
VcVLP2	26	485			56	106	134	277	144	7.4e-36	28	366	339	3.1e-98
VcGAP1	9	207					30	168	139	5.7e-25	12	199	188	5.1e-49
VcGAP2	19	280					23	161	139	6.9e-29	8	195	188	1.5e-50
VcGAP3	4	270			22	69	92	231	140	2.6e-25	14	265	252	2.9e-63
VcGAP4	21	382			37	86	116	240	125	2.2e-16	20	298	279	2.7e-68
VcGAP5	19	307			15	63	91	236	146	4.0e-24	7	281	275	2.6e-60
VcGAP6	16	284			17	67	88	215	128	3.3e-19	14	270	257	8.0e-55
VcGAP7	14	225 <sup>a</sup>					15	156	142	5.3e-29	4	212	209	9.2e-57
VcGAP8	5	369			64	113	141	281	141	4.6e-28	20	334	315	3.6e-84
VcGAP9	9	319 <sup>b</sup>			54	104	123	266	144	1.1e-28	38	306	269	5.5e-73
VcGAP10	5	233					30	166	137	1.6e-22	7	219	213	7.1e-45
VcGAP11	5	199					27	166	140	4.3e-19	8	198	191	5.7e-42
VcGAP12	8	402	21	48	79	131	159	296	138	3.3e-35	54	372	319	9.7e-91

481 The genomic coding sequence of VcRacGAP1 was obtained by genomic data mining. It comprised 9  
 482 exons with the CC region, C1 motif and RhoGAP domain encoded by exons 2 and 3, exons 5 and 6 and exon  
 483 7, respectively (Supplementary Table S7). In contrast to *Leptopilina*, the RhoGAP domain is encoded by a  
 484 single exon in *V. canescens* RacGAP1 as well as in all calyx RhoGAPs. Interestingly, the VcGAP12 gene is  
 485 located close to the VcRacGAP1 gene on chromosome 3, but is three exons shorter, suggesting a recent  
 486 incomplete duplication (Supplementary Table S7). However, no phylogenetic relationship could be inferred  
 487 between VcRacGAP1 and VcGAP12, as the corresponding proteins were either grouped in the phylogeny  
 488 but the grouping was not supported by bootstrap analysis (Figure 1D), or were not grouped in the  
 489 phylogeny (Supplementary Figures S4 and S5). In contrast to VcRacGAP1 and VcGAP12, VcVLP2 and the  
 490 other VcGAP genes are more widely distributed in the *V. canescens* genome, being organized into several  
 491 clusters consisting of two or more genes in tandem arrays (Figure 3 and Supplementary Table S7). For  
 492 several of these clusters, the *V. canescens* calyx RhoGAP proteins were found in bootstrap-supported  
 493 groups in the phylogeny, suggesting a close relationship (Figure 1D, Supplementary Figure S54 and Figure  
 494 3). This is the case, for example, for VcVLP2 and VcGAP9, VcGAP1 and VcGAP3, or VcGAP10 and VcGAP11,  
 495 which most likely originated from tandem duplication events. Therefore, it is possible that two or more  
 496 incomplete duplication events of the VcRacGAP1 gene, followed by further tandem and dispersed  
 497 duplication of the ancestrally duplicated genes, led to the current number of calyx RhoGAPs in *V.*  
 498 *canescens*.



499

500  
 501

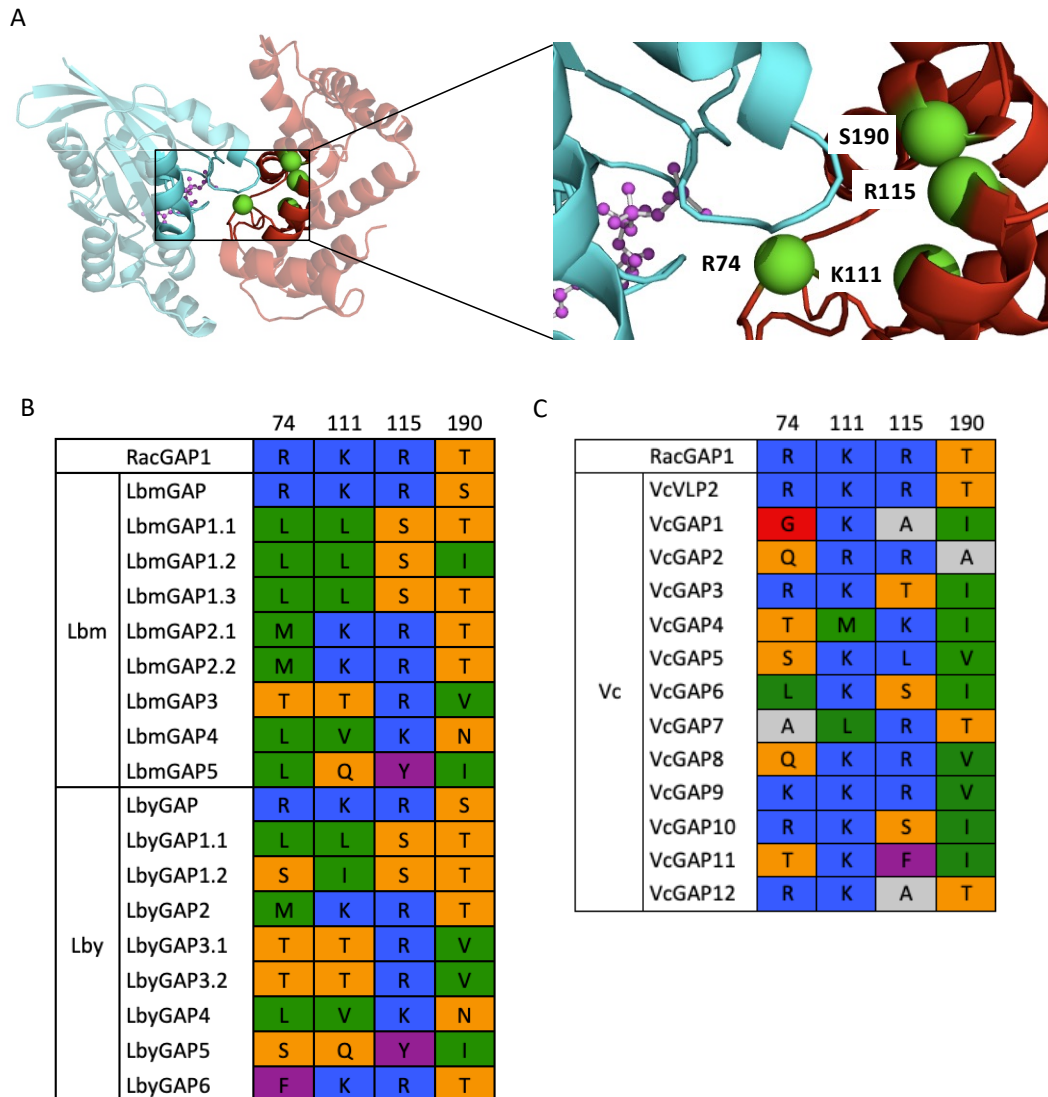
**Figure 3.** *V. canescens* chromosome map with the position of gene loci corresponding to RacGAP1 and calyx RhoGAPs visualized using chromoMap R package (Anand & Rodriguez Lopez 2022).

### 502 Evidence of positive selection in *L. bouvardi* venom and *V. canescens* calyx RhoGAP sequences

503 In a previous work, we identified four amino acid residues involved in the interaction of LbmGAP with  
 504 Rho GTPases (Colinet et al., 2007), including the key arginine residue (R74 in LbmGAP) required for the GAP  
 505 catalytic activity (Figure 4A). The other 8 venom RhoGAP sequences found in *L. bouvardi* Ism and ISy were  
 506 all mutated at this arginine residue (Figure 4B). Most also contained substitutions in one or more of the  
 507 other three amino acids involved in Rho GTPase interaction (Figure 4B). In *V. canescens*, no substitutions  
 508 were found for VcVLP2 at the key arginine residue or at any of the three amino acids involved in Rho GTPase  
 509 interaction (Figure 4C). In contrast, all other *V. canescens* calyx RhoGAP sequences, including VcGAP9, for  
 510 which a close relationship with VcVLP2 could be inferred from phylogenetic analysis and chromosomal  
 511 location, exhibit substitutions in one or more of the sites essential for GAP activity and/or involved in the  
 512 interaction with Rho GTPases (Figure 4C). These observations suggest that only LbmGAP (and its ortholog  
 513 LbyGAP) in *L. bouvardi* and VcVLP2 in *V. canescens* are functional as RhoGAPs.

514 Pairwise sequence identity was lower at the amino acid level than at the nucleotide level for both  
 515 *Leptopilina* venom RhoGAPs and *V. canescens* calyx RhoGAPs (Supplementary Figure S65). This indicates a  
 516 higher divergence at non-synonymous sites at the codon level compared to synonymous sites. A search for  
 517 positive selection at the codon level was performed to detect possible functional divergence of *L. bouvardi*  
 518 venom and *V. canescens* calyx RhoGAP sequences. PAML codon-based models with (M2a and M8) and  
 519 without (M1a and M7) selection were compared using likelihood ratio tests (LRTs). Both M1a/M2a and  
 520 M7/M8 comparisons resulted in the rejection of the null hypothesis suggesting that a fraction of codons in  
 521 RhoGAP sequences are under positive selection (Table 3).

522 Consistently, a total of 7 and 11 branches of the phylogenetic tree constructed with the *L. bouhardi*  
 523 venom and *V. canescens* calyx RhoGAP sequences, respectively, were detected by the REL branch-site test  
 524 as corresponding to lineages on which a subset of codons has evolved under positive selection (Figure 5A  
 525 and 6A). For *L. bouhardi*, 6 of the 7 lineages under positive selection were internal branches, indicating that  
 526 selection occurred primarily before the separation of the *L. bouhardi* Ism and ISy strains (Figure 5A).



527

528 **Figure 4. Substitutions in the essential sites for GAP activity and/or involved in interaction with Rho**  
 529 **GTPases** (A) Tertiary structure of LbmGAP (red) in complex with Rac1 (blue) and the transition-state  
 530 analogue GDP.AIF3 (modeled by homology for sequence spanning amino acid residues 51 to 216 in  
 531 Colinet et al., 2007). The four sites essential for GAP activity and/or involved in interaction with  
 532 RhoGTPases are colored green. (B) Amino acids found at the four sites essential for GAP activity  
 533 and/or involved in the interaction with RhoGTPases for *Leptopilina* RacGAP1 and *L. bouhardi* venom  
 534 RhoGAP sequences. The numbering corresponds to the positions in the LbmGAP sequence. (C) Amino  
 535 acids at the four sites essential for GAP activity and/or involved in interaction with RhoGTPases for  
 536 *V. canescens* RacGAP1 and calyx RhoGAP sequences. The numbering corresponds to the positions in  
 537 the LbmGAP sequence. In B and C, amino acids are colored according to their properties following  
 538 the RasMol amino acid color scheme.

539

540  
541  
542  
543  
544

**Table 3.** Positive selection analysis among sites using CodeML for *L. bouleardi* venom and *V. canescens* calyx RhoGAP sequences. lnL is the log likelihood of the model. p-value is the result of likelihood ratio tests (LRTs). Global  $\omega$  is the estimate of the dN/dS ratio under the model (given as a weighted average). Parameters ( $\omega > 1$ ) are parameters estimates for a dN/dS ratio greater than 1 ( $p$  is the proportion of sites with  $\omega > 1$ ).

<i>L. bouleardi</i>				
Model	lnL	p-value	Global $\omega$	Parameters ( $\omega > 1$ )
M1a: neutral	-5735.55		0.71	
M2a: selection	-5688.59	< 0.001	1.65	$\omega = 4.70, p = 0.21$
M7: $\beta$	-5741.07		0.70	
M8: $\beta$ & $\omega$	-5688.19	< 0.001	1.56	$\omega = 4.4, p = 0.22$
<i>V. canescens</i>				
Model	lnL	p-value	Global $\omega$	Parameters ( $\omega > 1$ )
M1a: neutral	-12616.14		0.78	
M2a: selection	-12574.17	< 0.001	1.31	$\omega = 2.72, p = 0.28$
M7: $\beta$	-12612.64		0.73	
M8: $\beta$ & $\omega$	-12564.70	< 0.001	1.21	$\omega = 2.30, p = 0.34$

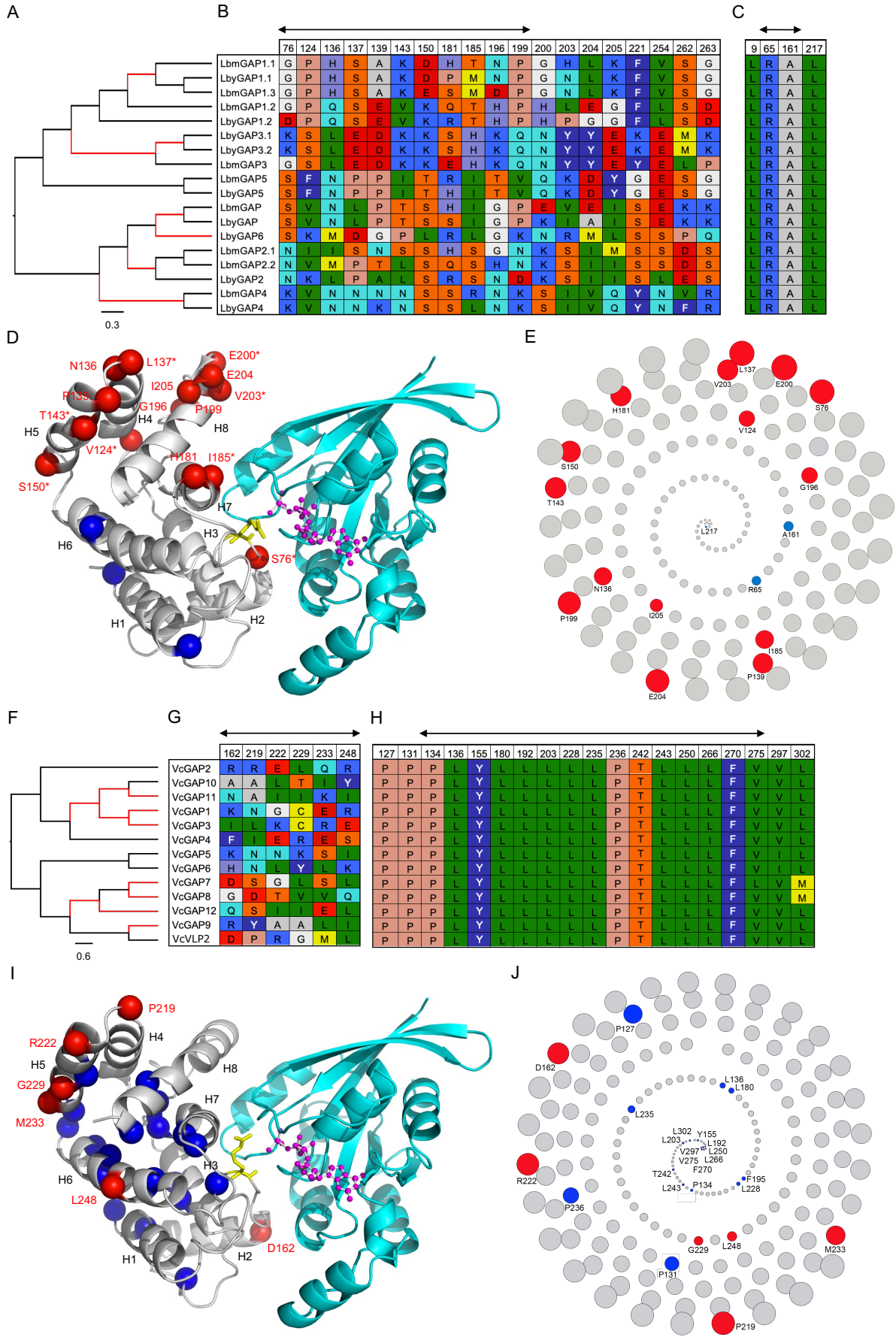
545

546 The combined use of five different methods identified a total of 19 codons as candidates under positive  
547 selection for the *L. bouleardi* venom RhoGAP sequences, most of which were found in the region  
548 corresponding to the RhoGAP domain (Figure 5B). In contrast, only 4 amino acids were detected as evolving  
549 under negative selection in the *L. bouleardi* venom RhoGAPs, respectively (Figure 5C). The leucine at position  
550 9 in LbmGAP is located in the signal peptide, demonstrating the importance of this region. The other three  
551 amino acids in *L. bouleardi* and most of those in *V. canescens* under negative selection are buried in the  
552 protein and are probably important for the structural stability (Figures 5D and 5E and Supplementary Figure  
553 S76A).

554 Interestingly, at least one radical change in charge and/or polarity of the corresponding amino acids  
555 was found for all selected codons (Figure 5B). For example, the polar uncharged serine residue at position  
556 76 in LbmGAP was replaced by a negatively charged lysine residue in LbmGAP4 (Figure 5B). Since radical  
557 changes are more likely to modify protein function than conservative changes, this suggests that the  
558 identified non-synonymous substitutions may be adaptive. Interestingly, the corresponding amino acids  
559 are mostly exposed on the surface of the protein and therefore likely to interact with partners (Figures 5D  
560 and 5E and Supplementary Figure S76A).

561 We therefore generated site-specific mutants of LbmGAP for 8 of the 19 amino acids under positive  
562 selection and compared their binding capabilities to Rho GTPases. Two-hybrid analysis revealed a lack of  
563 interaction for five of the mutants, indicating that the corresponding amino acids are essential for  
564 interaction with Rac GTPases (Table 4). On the other hand, the remaining three mutants were still able to  
565 interact strongly with Rac1 and Rac2, suggesting that the corresponding amino acids are not involved in  
566 the interaction with Rac GTPases (Table 4).

567 For the *V. canescens* calyx RhoGAP sequences, six amino acids were identified as candidates under  
568 positive selection and 19 under negative selection (Figures 5G and 5H). Four of the amino acids under  
569 positive selection are predicted to be exposed on the surface of the protein, indicating functional  
570 diversification in relation to interaction with partners as in *L. bouleardi* (Figures 5I and 5J and Supplementary  
571 Figure S76B). Most of the amino acids under negative selection are buried within the protein and are likely  
572 to be important for structural stability (Figures 5I and 5J and Supplementary Figure S76B).





574 **Figure 5. Identification of branches and codons under selection in *L. bouleari* venom RhoGAPs and**  
575 ***V. canescens* calyx RhoGAPs.** (A) Cladogram of *L. bouleari* venom RhoGAPs. (B) Codons under positive  
576 selection numbered according to LbmGAP amino acid sequence. (C) Codons under negative selection  
577 codons numbered according to LbmGAP amino acid sequence. (D) Sites under positive and negative  
578 selection displayed on the tertiary structure of LbmGAP (grey) in complex with Rac1 (blue) and the  
579 transition-state analogue GDP.AIF3 (modeled by homology for sequence spanning amino acid  
580 residues 51 to 216 in Colinet et al., 2007). A star indicates amino acid residues tested in mutagenesis  
581 and two-hybrid interaction assays. (E) Spiral view of LbmGAP amino acids in the order of their solvent  
582 accessibility. (F) Cladogram of *V. canescens* calyx RhoGAPs. (G) Codons under positive selection  
583 numbered according to VcVLP2 amino acid sequence. (H) Codons under negative selection numbered  
584 according to VcVLP2 amino acid sequence. (I) Sites under positive and negative selection displayed  
585 on the tertiary structure of VcVLP2 (grey) in complex with Rac1 (blue) and the transition-state  
586 analogue GDP.AIF3 (modeled by homology for sequence spanning amino acid residues 117 to 316).  
587 (J) Spiral view of VcVLP2 amino acids in the order of their solvent accessibility. In A and F, Branches  
588 identified under positive selection by the HyPhy BSR method are colored in red. The cladogram was  
589 rooted at midpoint. In B, C, G, and H, amino acids are colored according to their properties following  
590 the RasMol amino acid color scheme. The two-sided arrows indicate sites located in the RhoGAP  
591 domain. In D and I, the helices are shown as ribbons and numbered according to their location in the  
592 amino acid sequence of LbmGAP (D) or VcVLP2 (I). Sites under positive selection are displayed as red-  
593 colored spheres and numbered according to the LbmGAP (D) or VcVLP2 (I) sequence. Sites under  
594 negative selection are displayed as spheres and colored in blue. Protruding LbmGAP Arg74 (D) and  
595 VcVLP2 Arg156 (I) are shown as sticks and colored in yellow. GDP.AIF3 is shown as ball-and-sticks  
596 models and colored in magenta. In E and J, Most accessible amino acids come on the outermost ring of  
597 the spiral whereas the buried amino acids are occurring in the innermost ring. Radius of the circles  
598 corresponds to the relative solvent accessibility. Red and blue colors are used for amino acids under  
599 positive and negative selection respectively. All other amino acids are in grey.

600

601 **Table 4.** Summary of the results of interaction assays for the LbmGAP mutants. Results are based on  
602 growth on selective medium lacking histidine and qualitative  $\beta$ -galactosidase overlay assays. -: no  
603 interaction; (+): very weak interaction; +++: strong interaction. T: SV40 large T-antigen negative  
604 control.

	LbmGAP	LbmGAP S76K	LbmGAP V124K	LbmGAP L137D	LbmGAP T143L	LbmGAP S150L	LbmGAP I185K	LbmGAP E200G	LbmGAP V203R	T
Rac1	+++	-	-	+++	+++	+++	-	-	-	-
Rac2	+++	-	-	+++	+++	+++	-	-	-	-
CDC42	(+)	(+)	(+)	(+)	(+)	(+)	(+)	(+)	(+)	(+)
RhoA	-	-	-	-	-	-	-	-	-	-
Lamin	-	-	-	-	-	-	-	-	-	-

605

606

## Discussion

### 607 Independent convergent recruitment of vesicle-associated RhoGAP proteins in distantly related 608 parasitoid species

609 The process of duplication of a gene encoding a protein usually involved in a key physiological process  
610 whose function will be hijacked is a major mechanism of toxin recruitment (Fry et al., 2009; Wong & Belov  
611 2012; Casewell et al., 2013). The results of phylogeny and domain analyses indicate that the *Leptopilina*  
612 venom RhoGAPs and the calyx RhoGAPs found in *V. canescens* VLPs originated independently from the  
613 duplication of the gene encoding the cellular RacGAP1 in these species. The alternative hypothesis of a  
614 single initial duplication in the common ancestor of both *Leptopilina* and *V. canescens* would require  
615 numerous subsequent loss events since the last common ancestor of both *Leptopilina* and *V. canescens*  
616 dates back to the early radiation of parasitoid wasps (Peters et al., 2017). Furthermore, the presence of  
617 RhoGAP family proteins in the maternal fluids of parasitoid wasps has not been described outside of these  
618 species. This independent convergent recruitment may suggest a similar function in virulence in these two  
619 evolutionarily distant parasitoid species. Consistently, our results indicate that venom RhoGAPs in *L.*  
620 *bouleari* and *L. heterotoma* and calyx RhoGAPs in *V. canescens* are associated with extracellular vesicles,

621 named venosomes and VLPs, respectively. While these two types of vesicles have different tissue origins  
622 and formation mechanisms, *Leptopilina* venosomes and *V. canescens* VLPs would act as transport systems  
623 to deliver virulent proteins, including RhoGAPs, into host hemocytes to alter their function (Pichon et al.,  
624 2015; Wan et al., 2019). However, the role of RhoGAPs on host hemocytes is still unclear or even unknown,  
625 although we have previously shown that LbmGAP inactivates Rac-like GTPases (Colinet et al., 2007), which  
626 are required for successful encapsulation of *Leptopilina* eggs (Williams et al., 2005; Williams et al., 2006).

627 RacGAP1 is an intracellular multidomain protein consisting of a coiled-coil region followed by a C1 motif  
628 (protein kinase C-like zinc finger motif) and a RhoGAP domain (Tcherkezian & Lamane-Vane 2007).  
629 *Leptopilina* venom RhoGAPs, on the other hand, possess only a RhoGAP domain preceded by a secretory  
630 signal peptide. Sequence comparisons at the genomic level support the hypothesis of a single partial  
631 duplication of the RacGAP1 gene in the ancestor of the *Leptopilina* genus, resulting in the loss of a 5' portion  
632 of the sequence encoding the coiled-coil region and the C1 motif, followed by the acquisition of the signal  
633 peptide sequence. This initial evolutionary event would then have been followed by further duplication of  
634 the ancestral duplicate gene throughout the diversification of the genus *Leptopilina*, leading to the current  
635 number of venom RhoGAPs. A first hypothesis for the origin of the signal peptide would be that the loss of  
636 part of the 5' coding sequence in the duplicate resulted in a new N-terminal end for the encoded protein  
637 with signal peptide properties. Modification of the N-terminal end of the protein into a fully functional  
638 signal peptide may have required some point mutations after partial duplication, as in the case of the  
639 antifreeze protein of an Antarctic zoarcid fish (Deng et al., 2010). Another possibility is that the signal  
640 peptide originated from a process of partial duplication with recruitment (Katju & Lynch 2006), in which a  
641 "proto-peptide signal" coding sequence was acquired from the new genomic environment into which the  
642 partial copy was integrated. Finally, it is also possible that the new 5' region of the duplicated copy results  
643 from a chimeric duplication (Katju & Lynch 2006), e.g. from the partial duplication of another gene or by  
644 exon shuffling (Vibrantovski et al., 2006). The acquisition of the signal peptide probably facilitated the  
645 neofunctionalization of the venom RhoGAPs according to the evolutionary model of protein subcellular  
646 relocalization (PSR) proposed by Byun McKay & Geeta (2007), according to which a modification of the N-  
647 or C-terminal region of a protein can change its subcellular localization, by the loss or acquisition of a  
648 specific localization signal, and enable it to acquire a new function.

649 In *V. canescens*, the N-terminal region of the calyx RhoGAPs is more variable in length, with some  
650 proteins retaining the C1 motif upstream of the RhoGAP domain and one retaining a coiled-coil region  
651 upstream of the C1 motif. Most of the *V. canescens* calyx RhoGAPs were predicted to contain a nuclear  
652 localization signal, consistent with (i) the accumulation of VcVLP2 in the nucleus of the calyx cells prior to  
653 its association with the virus-derived VLPs (Pichon et al., 2015) and (ii) our results from a proteomic analysis  
654 indicating that all 13 calyx RhoGAPs are associated with VLPs. Human RacGAP1 has been described to  
655 localize to the cytoplasm and nucleus (Mishima et al., 2002), suggesting that *V. canescens* calyx RhoGAPs  
656 have retained the RacGAP1 nuclear localization signal, unlike *Leptopilina* venom RhoGAPs. One of the *V.*  
657 *canescens* calyx RhoGAP genes is located close to the RacGAP1 gene in the genome, suggesting a recent  
658 partial tandem duplication, although without support from phylogenetic analyses. The other genes, on the  
659 other hand, are scattered throughout the genome suggesting that they originate from one or more older  
660 duplication events of the RacGAP1 gene. In contrast to *Leptopilina*, it cannot be excluded that two or more  
661 partial duplication events of the RacGAP1-encoding gene occurred in *V. canescens*, followed by further  
662 duplication of ancestral duplicates.

### 663 **Accelerated evolution through duplication and divergence: pseudogenization and/or** 664 **neofunctionalization?**

665 Our work revealed a significant divergence for the two multigene families of RhoGAPs in *L. bouleardi*  
666 and *V. canescens* compared to RacGAP1, illustrated by the presence of substitutions on the arginine  
667 essential for GAP activity and/or on one or more of the amino acids shown to be important, or even  
668 necessary, for interaction with the Rac GTPases in all RhoGAPs except LbmGAP (and its ortholog LbyGAP)  
669 and VcVLP2. The presence of substitutions at key sites in the majority of *L. bouleardi* venom and *V. canescens*  
670 calyx RhoGAPs suggests a loss of function by pseudogenization. However, peptide matches were found in  
671 proteomic analyses for each of these RhoGAPs, indicating that the corresponding genes are successfully  
672 transcribed and translated. Furthermore, our results indicate that the ancestrally acquired secretory signal  
673 peptide, in which we identified an amino acid under negative selection, is conserved in all *L. bouleardi*

674 RhoGAPs and that most *V. canescens* RhoGAPs conserved the nuclear localization signal of RacGAP1. In  
675 addition, all RhoGAPs retained the ability to associate with vesicles, namely venosomes in *L. bouleari* and  
676 VLPs in *V. canescens*. Finally, we showed that several amino acids embedded in the protein structure  
677 evolved under negative selection, suggesting that they are important for protein stability. Taken together,  
678 these observations are not consistent with the hypothesis that any of the mutated RhoGAPs is undergoing  
679 a pseudogenization process, although it cannot be excluded that this process is quite recent and could have  
680 been initiated by the loss of the GAP active site.

681 An alternative hypothesis to pseudogenization would be functional diversification of the mutated  
682 RhoGAPs independent of the Rho pathway. Indeed, we have evidenced an evolution under positive  
683 selection for the majority of RhoGAPs in the two multigenic families. Most of the sites under positive  
684 selection are located on the surface of the protein and are therefore likely to interact with partners. In  
685 addition, directed mutagenesis and two-hybrid experiments in *L. bouleari* have shown that some of these  
686 amino acids are not involved in the interaction with Rac GTPases. Although the majority of studies on the  
687 RhoGAP domain concern the interaction with Rho GTPases, interactions with other proteins have also been  
688 described (Ban et al., 2004; Xu et al., 2013), supporting the hypothesis of a neofunctionalization of the  
689 mutated RhoGAPs. Further studies will be needed to determine which functions the mutated RhoGAPs  
690 have acquired in relation to parasitism. Recently, a possible role has been proposed for one of the RhoGAPs  
691 found in the venom of the ISy line of *L. bouleari* in the induction of reactive oxygen species (ROS) in the  
692 central nervous system of *D. melanogaster* in the context of superparasitism avoidance (Chen et al., 2021).  
693 However, ROS production is notably regulated by the GTPases Rac1 and Rac2 (Hobbs et al., 2014), whereas  
694 this venom protein (named EsGAP1 in Chen et al., 2021 and corresponding to LbyGAP6 in our study) has  
695 likely lost its RhoGAP activity due to a substitution on the arginine at position 74. Therefore, the mechanism  
696 by which EsGAP1 would be involved in ROS induction is unclear.

697 Other potential factors involved in parasitic success have been described previously that are encoded  
698 by large gene families and similarly correspond to truncated forms of cellular proteins that have retained  
699 only a single conserved domain, such as protein tyrosine phosphatases (PTPs) or viral ankyrins (V-ANKs) of  
700 bracoviruses. In the case of bracovirus PTPs, some are active as phosphatases, while others are mutated in  
701 their catalytic site and have been shown to be inactive as PTPs (Provost et al., 2004). In the latter case, as  
702 well as for V-ANK, it has been suggested that by binding to their target, they may act as constitutive  
703 inhibitors of the function of the corresponding cellular protein (Provost et al., 2004; Thoetkiattikul et al.,  
704 2005). Moreover, the model of adaptive evolution by competitive evolution of duplicated gene copies  
705 (Francino 2005) predicts that after a first step in which different copies explore the mutation space, once  
706 a protein with an optimal function is obtained, the other copies will begin to decay and undergo  
707 pseudogenization. This can lead to intermediate situations where both functional and non-functional  
708 proteins are produced, as observed for different virulence protein families of parasitoid wasps. Some of  
709 the described features of *L. bouleari* and *V. canescens* RhoGAPs may suggest that a process of competitive  
710 evolution is underway in *V. canescens* and *L. bouleari*, although our results are also consistent with the  
711 hypothesis of a possible neofunctionalization of these vesicle-associated proteins as discussed above.

712 In conclusion, we evidenced the independent convergent origin and accelerated evolution of a  
713 multigene family of vesicle-associated RhoGAP proteins in two unrelated parasitic wasps. Strikingly, these  
714 vesicles, which are similarly involved in parasitism, are produced in distinct organs: the venom apparatus  
715 in *Leptopilina* and the ovarian calyx in *V. canescens*. In the case of *Leptopilina* RhoGAPs, the acquisition of  
716 a secretory signal peptide after incomplete duplication of the RacGAP1 gene allowed secretion into the  
717 venom where the vesicles are formed. *V. canescens* RhoGAPs, on the other hand, probably retained the  
718 RacGAP1 nuclear localization signal, because it is in the nucleus of calyx cells that VLPs are formed. Another  
719 striking point is that our results suggest a possible functional diversification of vesicle-associated RhoGAPs  
720 in both species, with the exception of LbmGAP (and its ortholog LbyGAP) in *L. bouleari* and VcVLP2 in *V.*  
721 *canescens*, which are probably the only ones with RhoGAP activity. An open question would be whether all  
722 RhoGAPs are important for parasite success, but by different mechanisms, independent of the Rho  
723 pathway or not, depending on whether RhoGAPs are mutated or not.

724

725

## Acknowledgements

726 We are highly grateful to Christian Rebuf for help in insects rearing. We also thank Pr. M. T. Kimura  
727 (Hokkaido University, Japan) for providing biological material. We would also like to thank Anthony  
728 Bretaudeau (INRIA, Rennes, France) for help in the use of the workflows available at the BIPAA platform,  
729 the genotoul bioinformatics platform Toulouse Occitanie (Bioinfo Genotoul,  
730 <https://doi.org/10.15454/1.5572369328961167E12>) for providing computing resources and the BIG  
731 bioinformatics platform from the PlantBios infrastructure for providing facilities and technical support.

732

## Data and supplementary information availability

733 Raw data from the Illumina RNASeq sequencing of the *L. victoriana* venom apparatus are available at  
734 NCBI under the BioProject ID PRJNA974978.

735 The mass spectrometry proteomics data from *L. boulandi* and *L. heterotoma* venosomes have been  
736 deposited to the ProteomeXchange Consortium via the PRIDE (Perez-Riverol et al., 2022) partner repository  
737 with the dataset identifier PXD041695.

738 Supplementary information and material are available online at Data INRAE:  
739 <https://doi.org/10.57745/k82IWQ>

740

## Conflict of interest disclosure

741 The authors declare that they comply with the PCI rule of having no financial conflicts of interest in  
742 relation to the content of the article.

743 Jean-Luc Gatti and Marylène Poirié are recommenders of PCI Zoology.

744

## Funding

745 This work was supported by the Department of Plant Health and Environment from INRAE and the  
746 French Government (National Research Agency, ANR) through the “Investments for the Future” programs  
747 LABEX SIGNALIFE ANR-11-LABX-0028-01 and IDEX UCAJedi ANR-15-IDEX-01.

748

## References

749 Abd-Alla AM, Cousserans F, Parker AG, Jehle JA, Parker NJ, Vlak JM, Robinson AS, Bergoin M (2008) Genome  
750 analysis of a *Glossina pallidipes* salivary gland hypertrophy virus reveals a novel, large, double-stranded  
751 circular DNA virus. *Journal of Virology*, **82**, 4595-4611. <https://doi.org/10.1128/jvi.02588-07>

752 Anand L, Rodriguez Lopez CM (2022) ChromoMap: an R package for interactive visualization of multi-omics  
753 data and annotation of chromosomes. *BMC Bioinformatics*, **23**, 33. <https://doi.org/10.1186/s12859-021-04556-z>

754 Ban R, Irino Y, Fukami K, Tanaka H (2004) Human mitotic spindle-associated protein PRC1 inhibits  
755 MgcRacGAP activity toward Cdc42 during the metaphase. *Journal of Biological Chemistry*, **279**, 16394-  
757 16402. <https://doi.org/10.1074/jbc.m313257200>

758 Benkert P, Biasini M, Schwede T (2011) Toward the estimation of the absolute quality of individual protein  
759 structure models. *Bioinformatics*, **27**, 343-350. <https://doi.org/10.1093/bioinformatics/btq662>

760 Bézier A, Herbinière J, Lanzrein B, Drezen JM (2009) Polydnavirus hidden face: the genes producing virus  
761 particles of parasitic wasps. *Journal of Invertebrate Pathology*, **101**, 194-203.  
762 <https://doi.org/10.1016/j.jip.2009.04.006>

763 Brameier M, Krings A, MacCallum RM (2007) NucPred--predicting nuclear localization of proteins.  
764 *Bioinformatics*, **23**, 1159-1160. <https://doi.org/10.1093/bioinformatics/btm066>

765 Braunagel SC, Elton DM, Ma H, Summers MD (1996) Identification and analysis of an *Autographa californica*  
766 nuclear polyhedrosis virus structural protein of the occlusion-derived virus envelope: ODV-E56.  
767 *Virology*, **217**, 97-110. <https://doi.org/10.1006/viro.1996.0097>

768 Braunagel SC, Williamson ST, Saksena S, Zhong Z, Russell WK, Russell DH, Summers MD (2004) Trafficking  
769 of ODV-E66 is mediated via a sorting motif and other viral proteins: facilitated trafficking to the inner  
770 nuclear membrane. *Proceedings of the National Academy of Sciences*, **101**, 8372-8377.  
771 <https://doi.org/10.1073/pnas.0402727101>

772 Braunagel SC, Cox V, Summers MD (2009) Baculovirus data suggest a common but multifaceted pathway  
773 for sorting proteins to the inner nuclear membrane. *Journal of Virology*, **83**, 1280-1288.  
774 <https://doi.org/10.1128/jvi.01661-08>

775 Byun McKay SA, Geeta R (2007) Protein subcellular relocalization: A new perspective on the origin of novel  
776 genes. *Trends in Ecology & Evolution*, **22**, 338–344. <https://doi.org/10.1016/j.tree.2007.05.002>

777 Capella-Gutierrez S, Silla-Martinez JM, Gabaldon T (2009) trimAl: a tool for automated alignment trimming  
778 in large-scale phylogenetic analyses. *Bioinformatics*, **25**, 1972-1973.  
779 <https://doi.org/10.1093/bioinformatics/btp348>

780 Carton Y, Poirié M, Nappi AJ (2008) Insect immune resistance to parasitoids. *Insect Science*, **15**, 67-87.  
781 <https://doi.org/10.1111/j.1744-7917.2008.00188.x>

782 Casewell NR, Wüster W, Vonk FJ, Harrison RA, Fry BG (2013) Complex cocktails: the evolutionary novelty  
783 of venoms. *Trends in Ecology & Evolution*, **28**, 219-229. <https://doi.org/10.1016/j.tree.2012.10.020>

784 Chen S, Krinsky BH, Long M (2013) New genes as drivers of phenotypic evolution. *Nature Reviews Genetics*,  
785 **14**, 645-660. <https://doi.org/10.1038/nrg3521>

786 Chen J, Fang G, Pang L, Sheng Y, Zhang Q, Zhou Y, Zhou S, Lu Y, Liu Z, Zhang Y, Li G, Shi M, Chen X, Zhan S,  
787 Huang J (2021) Neofunctionalization of an ancient domain allows parasites to avoid intraspecific  
788 competition by manipulating host behaviour. *Nature Communications*, **12**, 5489.  
789 <https://doi.org/10.1038/s41467-021-25727-9>

790 Colinet D, Schmitz A, Depoix D, Crochard D, Poirié M (2007) Convergent use of RhoGAP toxins by eukaryotic  
791 parasites and bacterial pathogens. *PLoS Pathog* **3**: e203. <https://doi.org/10.1371/journal.ppat.0030203>

792 Colinet D, Schmitz A, Cazes D, Gatti J-L, and Poirié M (2010) The origin of intraspecific variation of virulence  
793 in an eukaryotic immune suppressive parasite. *PLoS Pathogens*, **6**, e1001206.  
794 <https://doi.org/10.1371/journal.ppat.1001206>

795 Colinet D, Deleury E, Anselme C, Cazes D, Poulain J, Azema-Dossat C, Belghazi M, Gatti J-L, Poirié M (2013)  
796 Extensive inter- and intraspecific venom variation in closely related parasites targeting the same host:  
797 the case of *Leptopilina* parasitoids of *Drosophila*. *Insect Biochemistry and Molecular Biology*, **43**, 601–  
798 611. <https://doi.org/10.1016/j.ibmb.2013.03.010>

799 Copley SD (2020) Evolution of new enzymes by gene duplication and divergence. *FEBS Journal*, **287**, 1262-  
800 1283. <https://doi.org/10.1111/febs.15299>.

801 de Graaf DC, Aerts M, Brunain M, Desjardins CA, Jacobs FJ, Werren JH, Devreese B (2010) Insights into the  
802 venom composition of the ectoparasitoid wasp *Nasonia vitripennis* from bioinformatic and proteomic  
803 studies. *Insect Molecular Biology*, **19**, 11-26. <https://doi.org/10.1111/j.1365-2583.2009.00914.x>

804 Deng C, Cheng C-HC, Ye H, He X, Chen L (2010) Evolution of an antifreeze protein by neofunctionalization  
805 under escape from adaptive conflict. *Proceedings of the National Academy of Sciences*, **107**, 21593-  
806 21598. <https://doi.org/10.1073/pnas.1007883107>

807 Delpont W, Poon AF, Frost SD, Kosakovsky Pond SL (2010) Datamonkey 2010: A suite of phylogenetic  
808 analysis tools for evolutionary biology. *Bioinformatics*, **26**, 2455-2477.  
809 <https://doi.org/10.1093/bioinformatics/btq429>

810 Drezen J-M, Chevignon G, Louis F, Hugué E (2014) Origin and evolution of symbiotic viruses associated  
811 with parasitoid wasps. *Current Opinion in Insect Science*, **6**, 35-43.  
812 <https://doi.org/10.1016/j.cois.2014.09.008>

813 Du J, Lin Z, Volovych O, Lu Z, Zou Z (2020) A RhoGAP venom protein from *Microplitis mediator* suppresses  
814 the cellular response of its host *Helicoverpa armigera*. *Developmental & Comparative Immunology*, **108**,  
815 103675. <https://doi.org/10.1016/j.dci.2020.103675>

816 Dupas S, Frey F, Carton Y (1998) A single parasitoid segregating factor controls immune suppression in  
817 *Drosophila*. *Journal of Heredity*, **89**, 306-311. <https://doi.org/10.1093/jhered/89.4.306>

818 Edgar RC (2004) Muscle: multiple sequence alignment with high accuracy and high throughput. *Nucleic  
819 Acids Research*, **32**, 1792–1797. <https://doi.org/10.1093/nar/gkh340>

820 Eddy SR (2009) A new generation of homology search tools based on probabilistic inference. *Genome  
821 Informatics*, **23**, 205–211. [https://doi.org/10.1142/9781848165632\\_0019](https://doi.org/10.1142/9781848165632_0019)

822 Feddersen I, Sander K, Schmidt O (1986) Virus-like particles with host protein-like antigenic determinants  
823 protect an insect parasitoid from encapsulation. *Experientia*, **42**, 1278-1281.  
824 <https://doi.org/10.1007/BF01946422>

825 Francino MP (2005) An adaptive radiation model for the origin of new gene functions. *Nature Genetics*, **37**,  
826 573-577. <https://doi.org/10.1038/ng1579>

827 Fromont-Racine M, Rain JC, Legrain P (1997) Toward a functional analysis of the yeast genome through  
828 exhaustive two-hybrid screens. *Nature Genetics*, **16**, 277-282. <https://doi.org/10.1038/ng0797-277>

829 Fry BG, Roelants K, Champagne DE, Scheib H, Tyndall JDA, King GF, Nevalainen TJ, Normann JA, Lewis RJ,  
830 Norton RS, Renjifo D, Rodriguez de la Vega RC (2009) The toxicogenomic multiverse: convergent  
831 recruitment of proteins into animal venoms. *Annual Review of Genomics and Human Genetics*, **10**, 483-  
832 511. <https://doi.org/10.1146/annurev.genom.9.081307.164356>

833 Gatti J-L, Schmitz A, Colinet D, Poirié M (2012) Diversity of virus-like particles in parasitoids' venom: viral  
834 or cellular origin? In: Beckage NE, Drezen J-M, editors, Parasitoid viruses, pp. 181-192, London:  
835 Academic Press. <https://doi.org/10.1016/B978-0-12-384858-1.00015-1>

836 Godfray HCJ (1994) Parasitoids: behavioral and evolutionary ecology (Vol. 67): Princeton University Press.  
837 <https://doi.org/10.2307/j.ctvs32rmp>

838 Goecks J, Mortimer NT, Mobley JA, Bowersock GJ, Taylor J, Schlenke TA (2013) Integrative approach reveals  
839 composition of endoparasitoid wasp venoms. *PLoS One*, **8**, e64125.  
840 <https://doi.org/10.1371/journal.pone.0064125>

841 Goldberg T, Hecht M, Hamp T, Karl T, Yachdav G, Ahmed N, Altermann U, Angerer P, Ansoerge S, Balasz K,  
842 Bernhofer M, Betz A, Cizmadija L, Do KT, Gerke J, Greil R, Joerdens V, Hastreiter M, Hembach K, Herzog  
843 M, Kalemanov M, Kluge M, Meier A, Nasir H, Neumaier U, Prade V, Reeb J, Sorokoumov A, Troshani I,  
844 Vorberg S, Waldruff S, Zierer J, Nielsen H, Rost B (2014) LocTree3 prediction of localization. *Nucleic Acids  
845 Research*, **42**, W350-355. <https://doi.org/10.1093/nar/gku396>

846 Guindon S, Dufayard JF, Lefort V, Anisimova M, Hordijk W, Gascuel O (2010) New algorithms and methods  
847 to estimate maximum-likelihood phylogenies: assessing the performance of PhyML 3.0. *Systematic  
848 Biology*, **59**, 307-321. <https://doi.org/10.1093/sysbio/syq010>

849 Haas BJ, Papanicolaou A, Yassour M, Grabherr M, Blood PD, Bowden J, Couger MB, Eccles D, Li B, Lieber M,  
850 MacManes MD, Ott M, Orvis J, Pochet N, Strozzi F, Weeks N, Westerman R, William T, Dewey CN,  
851 Henschel R, LeDuc RD, Friedman N, Regev A (2013) De novo transcript sequence reconstruction from  
852 RNA-seq using the Trinity platform for reference generation and analysis. *Nature Protocols*, **8**, 1494-  
853 1512. <https://doi.org/10.1038/nprot.2013.084>

854 Hobbs GA, Zhou B, Cox AD, Campbell SL (2014) Rho GTPases, oxidation, and cell redox control. *Small  
855 GTPases*, **5**, e28579. <https://doi.org/10.4161/sgtp.28579>

856 Hong T, Summers MD, Braunagel SC (1997) N-terminal sequences from *Autographa californica* nuclear  
857 polyhedrosis virus envelope proteins ODV-E66 and ODV-E25 are sufficient to direct reporter proteins  
858 to the nuclear envelope, intranuclear microvesicles and the envelope of occlusion derived virus.  
859 *Proceedings of the National Academy of Sciences*, **94**, 4050-4055.  
860 <https://doi.org/10.1073/pnas.94.8.4050>

861 Jancek S, Bézier A, Gayral P, Paillusson C, Kaiser L, Dupas S, Le Ru BP, Barbe V, Periquet G, Drezen J-M,  
862 Herniou E A (2013) Adaptive selection on bracovirus genomes drives the specialization of *Cotesia*  
863 parasitoid wasps. *PLoS One*, **8**, e64432. <https://doi.org/10.1371/journal.pone.0064432>

864 Jones P, Binns D, Chang H-Y, Fraser M, Li W, McAnulla C, McWilliam H, Maslen J, Mitchell A, Nuka G, Pesseat  
865 S, Quinn AF, Sangrador-Vegas A, Scheremetjew M, Yong S-Y, Lopez R, Hunter S (2014) InterProScan 5:  
866 genome-scale protein function classification. *Bioinformatics*, **30**, 1236-1240.  
867 <https://doi.org/10.1093/bioinformatics/btu031>

868 Kabsch W, Sander C (1983) Dictionary of protein secondary structure: pattern recognition of hydrogen-  
869 bonded and geometrical features. *Biopolymers*, **22**, 2577-2637.  
870 <https://doi.org/10.1002/bip.360221211>

871 Kalyanamoorthy S, Minh BQ, Wong TKF, von Haeseler A, Jermini LS (2017) ModelFinder: fast model  
872 selection for accurate phylogenetic estimates. *Nature Methods*, **14**, 587-589.  
873 <https://doi.org/10.1038/nmeth.4285>

874 Katju V, Lynch M (2006) On the formation of novel gene by duplication in the *Caenorhabditis elegans*  
875 genome. *Molecular Biology and Evolution*, **23**, 1056-1067. <https://doi.org/10.1093/molbev/msj114>

876 Katoh K, Standley DM (2013) MAFFT multiple sequence alignment software version 7: Improvements in  
877 performance and usability. *Molecular Biology and Evolution*, **30**, 772–780.  
878 <https://doi.org/10.1093/molbev/mst010>

879 Kelley LA, Mezulis S, Yates CM, Wass MN, Sternberg MJ (2015) The Phyre2 web portal for protein modeling,  
880 prediction and analysis. *Nature Protocols*, **10**, 845–858. <https://doi.org/10.1038/nprot.2015.053>

881 Kolde R (2019) pheatmap: Pretty Heatmaps. R package version 1.0.12. [https://CRAN.R-](https://CRAN.R-project.org/package=pheatmap)  
882 [project.org/package=pheatmap](https://CRAN.R-project.org/package=pheatmap)

883 Kosakovsky Pond SL, Frost SD (2005) Not so different after all: a comparison of methods for detecting  
884 amino acid sites under selection. *Molecular Biology and Evolution*, **22**, 1208–1222.  
885 <https://doi.org/10.1093/molbev/msi105>

886 Kosakovsky Pond SL, Murrell B, Fourment M, Frost SD, Delpont W, Scheffler K (2011) A random effects  
887 branch-site model for detecting episodic diversifying selection. *Molecular Biology and Evolution*, **28**,  
888 3033–3043. <https://doi.org/10.1093/molbev/msr125>

889 Labrosse C, Stasiak K, Lesobre J, Grangeia A, Huguet E, Drezen J-M, Poirié M (2005) A RhoGAP protein as a  
890 main immune suppressive factor in the *Leptopilina boulardi* (Hymenoptera, Figitidae)-*Drosophila*  
891 *melanogaster* interaction. *Insect Biochemistry and Molecular Biology*, **35**, 93–103.  
892 <https://doi.org/10.1016/j.ibmb.2004.10.004>

893 Lefort V, Longueville J-E, Gascuel O (2017) SMS : Smart model selection in PhyML. *Molecular Biology and*  
894 *Evolution*, **34**, 2422–2424. <https://doi.org/10.1093/molbev/msx149>

895 Long M, VanKuren NW, Chen S, Vibranovski MD (2013) New gene evolution: little did we know. *Annual*  
896 *Review of Genetics*, **47**, 307–333. <https://doi.org/10.1146/annurev-genet-111212-133301>

897 Lucas A, Van Dyke M, Stock J (1991) Predicting coiled coils from protein sequences. *Science*, **252**, 1162–  
898 1164. <https://doi.org/10.1126/science.252.5009.1162>

899 Magadum S, Banerjee U, Murugan P, Gangapur D, Ravikesavan R (2013) Gene duplication as a major force  
900 in evolution. *Journal of genetics*, **92**, 155–61. <https://doi.org/10.1007/s12041-013-0212-8>.

901 Millar AH, Whelan J, Small I (2006) Recent surprises in protein targeting to mitochondria and plastids.  
902 *Current Opinion in Plant Biology*, **9**, 610–615. <https://doi.org/10.1016/j.pbi.2006.09.002>

903 Minh BQ, Schmidt HA, Chernomor O, Schrempf D, Woodhams MD, von Haeseler A, Lanfear R (2020) IQ-  
904 TREE 2: New models and efficient methods for phylogenetic inference in the genomic era. *Molecular*  
905 *Biology and Evolution*, **37**, 1530–1534. <https://doi.org/10.1093/molbev/msaa015>

906 Mishima M, Kaitna S, Glotzer M (2002) Central spindle assembly and cytokinesis require a kinesin-like  
907 protein/RhoGAP complex with microtubule bundling activity. *Developmental Cell*, **2**, 41–54.  
908 [https://doi.org/10.1016/s1534-5807\(01\)00110-1](https://doi.org/10.1016/s1534-5807(01)00110-1)

909 Mueller JC, Andreoli C, Prokisch H, Meitinger T (2004) Mechanisms for multiple intracellular localization of  
910 human mitochondrial proteins. *Mitochondrion*, **3**, 315–325.  
911 <https://doi.org/10.1016/j.mito.2004.02.002>

912 Murrell B, Wertheim JO, Moola S, Weighill T, Scheffler K, Kosakovsky Pond SL (2012) Detecting individual  
913 sites subject to episodic diversifying selection. *PLoS Genetics*, **8**, e1002764.  
914 <https://doi.org/10.1371/journal.pgen.1002764>

915 Murrell B, Moola S, Mabona A, Weighill T, Sheward D, Kosakovsky Pond SL, Scheffler K (2013) FUBAR: A  
916 fast, unconstrained bayesian approximation for inferring selection. *Molecular Biology and Evolution*,  
917 **30**, 1196–1205. <https://doi.org/10.1093/molbev/mst030>

918 Nakai K, Horton P (1999) PSORT: a program for detecting sorting signals in proteins and predicting their  
919 subcellular localization. *Trends in Biochemical Sciences*, **24**, 34–36. [https://doi.org/10.1016/s0968-](https://doi.org/10.1016/s0968-0004(98)01336-x)  
920 [0004\(98\)01336-x](https://doi.org/10.1016/s0968-0004(98)01336-x)

921 Novković B, Mitsui H, Suwito A, Kimura MT (2011) Taxonomy and phylogeny of *Leptopilina* species  
922 (Hymenoptera: Cynipoidea: Figitidae) attacking frugivorous drosophilid flies in Japan, with description  
923 of three new species. *Entomological Science*, **14**, 333–346. [https://doi.org/10.1111/j.1479-](https://doi.org/10.1111/j.1479-8298.2011.00459.x)  
924 [8298.2011.00459.x](https://doi.org/10.1111/j.1479-8298.2011.00459.x)

925 Ohno S (1970) Evolution by gene duplication. Springer Verlag, Berlin. [https://doi.org/10.1007/978-3-642-](https://doi.org/10.1007/978-3-642-86659-3)  
926 [86659-3](https://doi.org/10.1007/978-3-642-86659-3)

927 Pennacchio F, Strand MR (2006) Evolution of developmental strategies in parasitic Hymenoptera. *Annual*  
928 *Review of Entomology*, **51**, 233–258. <https://doi.org/10.1146/annurev.ento.51.110104.151029>

929 Perez-Riverol Y, Bai J, Bandla C, Hewapathirana S, García-Seisdedos D, Kamatchinathan S, Kundu D, Prakash  
930 A, Frericks-Zipper A, Eisenacher M, Walzer M, Wang S, Brazma A, Vizcaíno JA (2022). The PRIDE  
931 database resources in 2022: A Hub for mass spectrometry-based proteomics evidences. *Nucleic Acids*  
932 *Research*, **50**, D543-D552. <https://doi.org/10.1093/nar/gkab1038>  
933 Peters RS, Krogmann L, Mayer C, Donath A, Gunkel S, Meusemann K, Kozlov A, Podsiadlowski L, Petersen  
934 M, Lanfear R, Diez PA, Heraty J, Kjer KM, Klopstein S, Meier R, Polidori C, Schmitt T, Liu S, Zhou X,  
935 Wappler T, Rust J, Misof B, Niehuis O (2017) Evolutionary history of the Hymenoptera. *Current Biology*,  
936 **27**, 1013-1018. <https://doi.org/10.1016/j.cub.2017.01.027>  
937 Pichon A, Bézier A, Urbach S, Aury J-M, Jouan V, Ravallec M, Guy J, Cousserans F, Thézé J, Gauthier J,  
938 Demettre E, Schmieder S, Wurmser F, Sibut V, Poirié M, Colinet D, da Silva C, Couloux A, Barbe V, Drezen  
939 J-M, Volkoff A-N (2015) Recurrent DNA virus domestication leading to different parasite virulence  
940 strategies. *Science Advances*, **1**, e1501150. <https://doi.org/10.1126/sciadv.1501150>  
941 Poirié M, Carton Y, Dubuffet A (2009) Virulence strategies in parasitoid Hymenoptera as an example of  
942 adaptive diversity. *Comptes Rendus Biologies*, **332**, 311–320.  
943 <https://doi.org/10.1016/j.crvi.2008.09.004>  
944 Poirié M, Colinet D, Gatti J-L (2014) Insights into function and evolution of parasitoid wasp venoms. *Current*  
945 *Opinion in Insect Science*, **6**, 52–60. <https://doi.org/10.1016/j.cois.2014.10.004>  
946 Provost B, Varricchio P, Arana E, Espagne E, Falabella P, Huguet E, La Scaleia R, Cattolico L, Poirié M, Malva  
947 C, Olszewski JA, Pennacchio F, Drezen JM (2004) Bracoviruses contain a large multigene family coding  
948 for protein tyrosine phosphatases. *Journal of Virology*, **78**, 13090-13103.  
949 <https://doi.org/10.1128/jvi.78.23.13090-13103.2004>  
950 Rago, A, Gilbert DG, Choi J-H, Sackton TB, Wang X, Kelkar YD, Werren JH, Colbourne JK (2016) OGS2:  
951 genome re-annotation of the jewel wasp *Nasonia vitripennis*. *BMC Genomics*, **17**, 678.  
952 <https://doi.org/10.1186/s12864-016-2886-9>  
953 Reineke A, Asgari S, Schmidt O (2006) Evolutionary origin of *Venturia canescens* virus-like particles. *Archives*  
954 *of Insect Biochemistry and Physiology*, **61**, 123–133. <https://doi.org/10.1002/arch.20113>  
955 Serbielle C, Chowdhury S, Pichon S, Dupas S, Lesobre J, Purisima E, Drezen J-M, Huguet E (2008) Viral  
956 cystatin evolution and three-dimensional structure modelling: a case of directional selection acting on  
957 a viral protein involved in a host-parasitoid interaction. *BMC Biology*, **6**, 38.  
958 <https://doi.org/10.1186/1741-7007-6-38>  
959 Serbielle C, Dupas S, Perdereau E, Héricourt F, Dupuy C, Huguet E, Drezen, J-M (2012) Evolutionary  
960 mechanisms driving the evolution of a large polydnavirus gene family coding for protein tyrosine  
961 phosphatases. *BMC Ecology and Evolution*, **12**, 253. <https://doi.org/10.1186/1471-2148-12-253>  
962 Sievers F, Higgins DG (2018) Clustal Omega for making accurate alignments of many protein sequences.  
963 *Protein Science*, **27**, 135-145. <https://doi.org/10.1002/pro.3290>  
964 Slater GSC, Birney E (2005) Automated generation of heuristics for biological sequence comparison. *BMC*  
965 *Bioinformatics*, **6**, 31. <https://doi.org/10.1186/1471-2105-6-31>  
966 Stern A, Doron-Faigenboim A, Erez E, Martz E, Bacharach E, Pupko T (2007) Selecton 2007: advanced  
967 models for detecting positive and purifying selection using a Bayesian inference approach. *Nucleic Acids*  
968 *Research*, **35**(Web Server issue), W506-511. <https://doi.org/10.1093/nar/gkm382>  
969 Tcherkezian J, Lamarche-Vane N (2007). Current knowledge of the large RhoGAP family of proteins. *Biology*  
970 *of the Cell*, **99**, 67–86. <https://doi.org/10.1042/bc20060086>  
971 Thoetkiattikul H, Beck MH, Strand MR (2005) Inhibitor kappaB-like proteins from a polydnavirus inhibit NF-  
972 kappaB activation and suppress the insect immune response. *Proceedings of the National Academy of*  
973 *Sciences*, **102**, 11426-11431. <https://doi.org/10.1073/pnas.0505240102>  
974 Vibanovski MD, Sakabe NJ, de Souza SJ (2006) A possible role of exon-shuffling in the evolution of signal  
975 peptides of human proteins. *FEBS Letters*, **580**, 1621–1624.  
976 <https://doi.org/10.1016/j.febslet.2006.01.094>  
977 Wan B, Goguet E, Ravallec M, Pierre O, Lemauf S, Volkoff A-N, Gatti J-L, Poirié M (2019) Venom atypical  
978 extracellular vesicles as interspecies vehicles of virulence factors involved in host specificity: the case  
979 of a drosophila parasitoid wasp. *Frontiers in Immunology*, **10**, 1688.  
980 <https://doi.org/10.3389/fimmu.2019.01688>  
981 Wickham H (2009) Ggplot2: Elegant graphics for data analysis. 2nd Edition, Springer, New York.  
982 <https://doi.org/10.1007/978-0-387-98141-3>



983 Wickham H, François R, Henry L, Müller K, Davis Vaughan (2023) dplyr: A grammar of data manipulation. R  
984 package version 1.1.0. <https://CRAN.R-project.org/package=dplyr>

985 Williams MJ, Ando I, Hultmark D (2005) *Drosophila melanogaster* Rac2 is necessary for a proper cellular  
986 immune response. *Genes to Cells*, **10**, 813–823. <https://doi.org/10.1111/j.1365-2443.2005.00883.x>

987 Williams MJ, Wiklund ML, Wikman S, Hultmark D (2006) Rac1 signalling in the *Drosophila* larval cellular  
988 immune response. *Journal of Cell Science*, **119**, 2015–2024. <https://doi.org/10.1242/jcs.02920>

989 Wong ESW, Belov K (2012) Venom evolution through gene duplications. *Gene*, **13**, 59–69.  
990 <https://doi.org/10.1016/j.gene.2012.01.009>

991 Xu J, Zhou X, Wang J, Li Z, Kong X, Qian J, Hu Y, Fang J-Y (2013) RhoGAPs attenuate cell proliferation by  
992 direct interaction with p53 tetramerization domain. *Cell Reports*, **3**, 1526-1538.  
993 <https://doi.org/10.1016/j.celrep.2013.04.017>

994 Yang Z (1997) PAML: a program package for phylogenetic analysis by maximum likelihood. *Bioinformatics*,  
995 **13**, 555-556. <https://doi.org/10.1093/bioinformatics/13.5.555>

996 Yang Z (2007) PAML 4: phylogenetic analysis by maximum likelihood. *Molecular Biology and Evolution*, **24**,  
997 1586-1591. <https://doi.org/10.1093/molbev/msm088>

998 Yang Z, Nielsen R, Goldman N, Pedersen AM (2000) Codon-substitution models for heterogeneous  
999 selection pressure at amino acid sites. *Genetics*, **155**, 431-449.  
1000 <https://doi.org/10.1093/genetics/155.1.431>

1001 Yang Z, Wong WS, Nielsen R (2005) Bayes empirical bayes inference of amino acid sites under positive  
1002 selection. *Molecular Biology and Evolution*, **22**, 1107–1118. <https://doi.org/10.1093/molbev/msi097>

1003 Zhang J (2000) Rates of conservative and radical nonsynonymous nucleotide substitutions in mammalian  
1004 nuclear genes. *Journal of Molecular Evolution*, **50**, 56–68. <https://doi.org/10.1007/s002399910007>